Send Orders for Reprints to reprints@benthamscience.net

Current Medicinal Chemistry, 2021, *28*, 7614-7633

REVIEW ARTICLE

Protein-Ligand Docking Simulations with AutoDock4 Focused on the Main Protease of SARS-CoV-2

Walter Filgueira de Azevedo Junior[1,2,*], Gabriela Bitencourt-Ferreira[1], Joana Retzke Godoy[1], Hilda Mayela Aran Adriano[3], Wallyson André dos Santos Bezerra[4] and Alexandra Martins dos Santos Soares[4]

[1]Pontifical Catholic University of Rio Grande do Sul (PUCRS), Av. Ipiranga, 6681 Porto Alegre/RS 90619-900, Brazil; [2]Specialization Program in Bioinformatics, Pontifical Catholic University of Rio Grande do Sul (PUCRS), Av. Ipiranga, 6681 Porto Alegre/RS 90619-900, Brazil; [3]Universidad de Celaya, Carretera Panamericana, Rancho Pinto km 269, 38080 Celaya, Gto. Zip Code 38080, Guanajuato, Mexico; [4]Department of Chemical Engineering, Federal University of Maranhão, Avenida dos Portugueses, 1966 São Luís / MA 65080-805, Brazil

Abstract: ***Background*:** The main protease of SARS-CoV-2 (M^{pro}) is one of the targets identified in SARS-CoV-2, the causative agent of COVID-19. The application of X-ray diffraction crystallography made available the three-dimensional structure of this protein target in complex with ligands, which paved the way for docking studies.

***Objective*:** Our goal here is to review recent efforts in the application of docking simulations to identify inhibitors of the M^{pro} using the program AutoDock4.

***Methods*:** We searched PubMed to identify studies that applied AutoDock4 for docking against this protein target. We used the structures available for M^{pro} to analyze intermolecular interactions and reviewed the methods used to search for inhibitors.

***Results*:** The application of docking against the structures available for the M^{pro} found ligands with an estimated inhibition in the nanomolar range. Such computational approaches focused on the crystal structures revealed potential inhibitors of M^{pro} that might exhibit pharmacological activity against SARS-CoV-2. Nevertheless, most of these studies lack the proper validation of the docking protocol. Also, they all ignored the potential use of machine learning to predict affinity.

***Conclusion*:** The combination of structural data with computational approaches opened the possibility to accelerate the search for drugs to treat COVID-19. Several studies used AutoDock4 to search for inhibitors of M^{pro}. Most of them did not employ a validated docking protocol, which lends support to critics of their computational methodology. Furthermore, one of these studies reported the binding of chloroquine and hydroxychloroquine to M^{pro}. This study ignores the scientific evidence against the use of these antimalarial drugs to treat COVID-19.

ARTICLE HISTORY

Received: December 23, 2020
Revised: February 24, 2021
Accepted: February 25, 2021

DOI:
10.2174/0929867328666210329094111

Keywords: COVID-19, SARS-CoV-2, protein-ligand interaction, autoDock4, docking, machine learning, main protease.

*Address correspondence to this author at the Pontifical Catholic University of Rio Grande do Sul (PUCRS), Av. Ipiranga, 6681 Porto Alegre/RS 90619-900, Brazil; Specialization Program in Bioinformatics, Pontifical Catholic University of Rio Grande do Sul (PUCRS), Av. Ipiranga, 6681 Porto Alegre/RS 90619-900 Brazil; Tel/Fax: +55-51-3320-3545; E-mails: walter.junior@pucrs.br; walter@azevedolab.net

1875-533X/21 $65.00+.00 © 2021 Bentham Science Publishers

Current Medicinal Chemistry

1. INTRODUCTION

Humanity has been caught by surprise with the SARS-CoV-2 infection, the etiological agent of COVID-19 [1-5]. This pandemic outbreak has affected millions worldwide. In many countries, COVID-19 harmed public health systems and the economy [6, 7].

This outbreak also worsened due to instances of the denial of the science practiced by some governments. Most notably, the Brazilian government position against the wearing of face masks and promoting public gatherings without the necessary precautions [8-14]. These outrageous positions against scientific evidence supporting social distancing during the COVID-19 pandemic claimed the lives of thousands [7]. Also, the lack of support to the preventive health measures increased the negative economic impact in an already impoverished population with a declining gross domestic product forecast for the coming years [15].

Furthermore, some governments strongly supported chloroquine and hydroxychloroquine to treat COVID-19 [11-14]. This indication has no scientific support. A definitive view against chloroquine and hydroxychloroquine to treat COVID-19 has been researched earlier [16]. Due to the urgent need for treatments and shots for COVID-19, many academic laboratories and pharmaceutical companies started developing vaccines [17] and drugs [18]. Among the protein targets identified in SARS-CoV-2 for drug discovery, the proteases received special attention [19]. The focus on proteases directed the studies to elucidate the structure of the main protease (3C-like proteinase) of SARS-CoV-2 (EC 3.4.22.69) (M^{pro}) in complex with several different ligands bound to the active site of this protein target [20-22]. This data paved the way for structure-based drug design (SBDD) efforts focused on this enzyme.

Projects using SBDD have the potential to speed-up the drug design through the identification of the structural features necessary for binding affinity [23-25]. One of the most successful uses of SBDD is the discovery of HIV-1 protease (EC 3.4.23.16) inhibitors and their therapeutical use to treat HIV infection [26]. The availability of structural data is a favorable scenario for protein-ligand docking simulations focused on the M^{pro}. Due to the apparent easiness in the use of docking programs, several research groups started precipitated screens without validation of the docking protocols and with no use of state-of-art computational approaches to build targeted-scoring functions using machine learning techniques. Machine learning models to predict protein-ligand binding affinity have shown superior predictive performance [27-37] compared to classical scoring functions available in docking programs such as AutoDock4 [38, 39].

In this review, we describe the structural data available for M^{pro}. We focus on intermolecular interactions and give an overview of the AutoDock4 scoring function. We analyze the application of AutoDock4 to screen potential inhibitors of the M^{pro} and evaluate the methodologies used by several different research groups in their virtual screening studies. We also highlight the potential of integrating machine learning techniques to build targeted-scoring functions for the M^{pro}.

2. METHODS

In the year 2020, the protein data bank (PDB) [40-42] reached over 170 k structures (search carried out on December 3, 2020). This structural data adds to the information about protein-ligand binding affinity and thermodynamic parameters. This binding-affinity data is available at BindingDB [43, 44], Binding MOAD (Mother of All Databases) [45-47], and PDBbind [48, 49]. PDB has an integration with these databases, which makes it possible to carry out searches to retrieve crystal structures for which experimental binding affinity data are available.

2.1. Crystallographic Structures

We searched for the structures of M^{pro} available at the PDB (search performed on December 3, 2020). We filtered the data for binding affinity information, specifically inhibition constant (K_i), inhibitory constant at 50% (IC_{50}), dissociation constant (K_d), and Gibbs free energy of binding for protein-ligand complexes (ΔG). We also filtered the structures to consider only those with X-ray diffraction crystallographic resolution better than 1.5 Å. We used the program SAnDReS [50, 51] to carry out data filtering and statistical analysis of the structures of the M^{pro}. We also employed the program SAnDReS to generate a graphical representation of the intermolecular interactions for selected structural data of M^{pro} with bound ligands. We used LigPlot+ [52, 53] to create 2D plots of van der Waals contacts and intermolecular hydrogen bonds for selected structures of M^{pro} complexed with ligands.

The program LigPlot+ allows defining structural criteria to determine protein-ligand interactions. It brings uniformity in the study of intermolecular interactions since it employs the same robust structural proof to identify a given contact for a pair of atoms. We analyzed each entry in the structural dataset to find additio-

nal data highlighting that the ligand found in the structure has inhibition activity. Where available, we used the information in the paper describing the data at the PDB since information related to binding affinity was not available.

2.2. AutoDock4 Scoring Function

Amongst the diverse group of theoretical methods used in receptor-ligand docking programs to estimate binding affinity, the empirical free energy scoring function implemented in the program AutoDock4 [38, 39] is one of the most effective in virtual screens for drug discovery. A search performed on PubMed using as strings protein, drug, and AutoDock returned 804 papers (search carried out on December 3, 2020). This result shows the influence of AutoDock4 to calculate the potential energy of receptor-ligand complexes and its application in the screening of new drugs. The AutoDock4 expression to estimate the energetics of protein-ligand systems has the following equation:

$$E_{RL} = \alpha_{LJ}\sum_{i,j}\left(\frac{A_{ij}}{r_{ij}^{12}} - \frac{B_{ij}}{r_{ij}^{6}}\right) + \alpha_{HB}\sum_{i,j}E(t)\left(\frac{C_{ij}}{r_{ij}^{12}} - \frac{D_{ij}}{r_{ij}^{10}}\right) + \alpha_{Desol}\sum_{i,j}\left(S_iV_j + S_jV_i\right)e^{-r_{ij}^2/2\sigma^2} + \alpha_{Torsion}0 + \alpha_{Electro}\sum_{i,j}\frac{q_iq_j}{\varepsilon(r_{ij})r_{ij}} \quad (1)$$

where E_{RL} is the total potential energy of the biological system involving a receptor (macromolecule) and a small organic molecule (ligand), and the α's correspond to the relative weights of each energy term. By small organic molecules, we mean ligands with molecular weight up to 500, for instance, those satisfying Lipinski's rule of five [54]. Originally these weights in equation (**1**) were determined through regression methods against a dataset of protein-ligand complexes with binding-affinity data.

The first term on the right side of equation (**1**) represents the dispersal/repulsion interactions (Lennard-Jones potential energy) [55]. In the above equation, r_{ij} denotes the interatomic distance involving atoms from the receptor and ligand. In the following term, we see an adjustment of the equation of Lennard-Jones potential. This adaptation is frequently applied to estimate hydrogen-bond energetics and uses a 10/12 potential function. The third term represents the desolvation potential and considers the volume of atoms (V_i or V_j) times a solvation parameter (S_i or S_j) and an exponential function with a fixed distance weight (σ = 3.5 Å). The following term considers the number of torsion angles ($N_{Torsion}$) present in the ligands. The final part of the equation (**1**) denotes the electrostatic potential energy, where we use the atomic partial charges (q_i and q_j) and the permittivity function $\varepsilon(r_{ij})$.

AutoDock4 employs the partial equalization of orbital electronegativity (PEOE) algorithm to evaluate atomic charges [38, 39]. In equation (**1**), the summations consider all pairs of ligand atoms (i) and receptor atoms (j) besides all those that are apart by three or more bonds. AutoDock4 employs equation (**1**) to estimate the pose binding affinity and chooses the lowest-binding affinity pose in receptor-ligand docking screens. The AutoDock4 uses data from the AMBER force field [56, 57] for the parameters used in equation (**1**) (A_{ij}, B_{ij}, C_{ij}, D_{ij}, V_i, V_j, S_i, and S_j). AMBER is a computational method to estimate the energetics of biomolecular systems. A search performed on PubMed using the terms force field and AMBER generated 1035 results (search carried out on December 3, 2020). This result shows the importance of AMBER calculate the potential energy of receptor-ligand complexes and its use for molecular dynamics simulations of macromolecules.

Calculation of $\varepsilon(r_{ij})$ for receptor-ligand structures is still a challenge. We have a wide range of methods to address the permittivity function for protein-ligand complexes [38, 39]. AutoDock4 estimates $\varepsilon(r_{ij})$ employing a sigmoidal distance-dependent permittivity function. This calculation uses the model suggested by Mehler and Solmajer [58]. The expression of the Mehler-Solmajer method for the permittivity function has the following form:

$$\varepsilon(r) = A + \frac{B}{1+ke^{-\lambda Br}} \quad (2)$$

In the implementation of equation (**2**) in the program AutoDock4, the parameters have the following values: $B = \varepsilon_r - A$; ε_r (the relative permittivity constant of bulk water at 25˚C) = 78.4; A = -8.5525, λ = 0.003627 and k = 7.7839 (standard permittivity function parameters).

Estimation of permittivity employing a value of ε_r =78.4 is appropriate for some biomolecular systems [59]. Nevertheless, we have reports of a wide range of

values used to estimate relative permittivity in computational studies of receptor-ligand interactions [60-67].

2.3. Search Algorithms Available in AutoDock4

AutoDock4 has four search algorithms available for receptor-ligand docking simulations. They are local search (LS), simulated annealing (SA), genetic algorithm (GA), and Lamarckian genetic algorithm (LGA). Most of the recent applications of AutoDock4 rely on the LGA. Nevertheless, depending on the protein-ligand structure, we can achieve relative success with all of them [38, 39].

2.4. Searches on PubMed

To have access to works describing the application of AutoDock4 to screen potential inhibitors of M^{pro}, we searched PubMed using strings in the following combination: AutoDock, SARS-CoV-2, and protease. We eliminated the AutoDock Vina studies of the search to focus on one docking program (AutoDock4). We named the results of this search as Search 1. We carried out another exploration of PubMed by adding the strings "machine learning" and "deep learning" to the previous search using the operator AND. We called the results of these searches Search 2 and 3. Also, we checked docking results reporting the potential binding of chloroquine and hydroxychloroquine to M^{pro}. We named them Search 4 and 5, respectively. The use of AutoDock4 with molecular dynamics simulations was searched and named Search 6. We gathered these results on December 3, 2020.

3. RESULTS AND DISCUSSION

3.1. Structural Data

A search on PDB using the FASTA sequence of M^{pro} (PDB access code: 7D1M) [68] returned a total of 230 structures with 100% identity with the probe, all determined using diffraction data. Further filtering of the dataset taking only PDBs for which experimental binding affinity data were available for K_i, K_d, IC_{50}, or ΔG returned none. However, we have affinity data for 150 ligands at BindingDB (a search carried out on December 3, 2020). These ligands still did not have structural data at PDB. We applied additional filtering with the crystallographic resolution criterion, using structures solved with data better than 1.5 Å. This procedure returned 36 high-resolution crystal structures. Among these crystal structures, one had no ligand bound to the protein, and we deleted it from the dataset (PDB access code: 7KPH). Table **1** shows the PDB access codes for these structures. We named these structures HRM^{pro} (high-resolution main protease of SARS--CoV-2 dataset).

Analysis of the crystallographic information of HRM^{pro} indicated that the resolution ranges from 1.2 to 1.48 Å. The highest resolution structure is the M^{pro} in complex with dimethyl sulfoxide (DMSO) (PDB access code: 7K3T). DMSO is a co-factor usually used in crystallization conditions [69-71]. This structure (7K3T) also showed the lowest values of B-factors. Such low values of B-factor indicate the definition of the electron density maps [72]. Another method used to evaluate the quality of a structure using X-ray diffraction crystallography is the root mean square deviation from the ideal geometry. Considering this feature, among the entries in the HRM^{pro}, the structure 5RFV shows the best overall performance. This structure has a covalent ligand with information about inhibition (1-[4-(thiophene-2-carbonyl) piperazin-1-yl] ethan-1-one) and DMSO. Specifically, for complexes with inhibitors, the highest resolution entry is the M^{pro} complex with GRL-2420 (PDB access code: 7JKV).

In Table **1**, we have additional information highlighting the entries for which the authors of the deposition of atomic coordinates made clear that the structures had an inhibitor bound to the complex. Although the PDB has an interface with BindingDB, Binding MOAD, and PDBbind, as we previously highlighted,

Table 1. PDB access codes of crystallographic structures of HRM^{pro}.

Type of ligand in the structure	PDB access codes
Co-factors used in the crystallization conditions (glycerol, DMSO, and 1,2-ethanediol)	7AR5, 7AR6, 6YB7, 6Y84, 5R8T, 7K3T, 6XKH
Non-covalent ligands bound to the active site	5RGK, 5RGW, 5RF6, 5R82, 5RFE
Non-covalent ligands bound to alternative sites	5RF8, 5RGJ, 5RED, 5RGR, 5RF9, 5RH4, 5RFD, 5RFB, 5RFC
Non-covalent allosteric inhibitors	7AWR, 7AXM
Covalent inhibitors bound to the active site	5RFV, 5RFW, 5RHB, 6XR3, 6XBG, 6XHM, 5RL2, 7K40, 6WNP, 7D1M, 7K6D, 7JKV

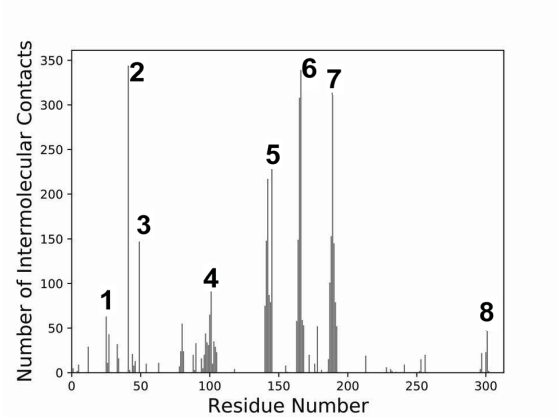

Fig. (1). Intermolecular interactions for 28 crystallographic structures of M^{pro} for which ligands are present in the complexes (PDB access codes: 7AWR, 5RGK, 5RF8, 5RGW, 5RF6, 5R82, 5RFE, 5RGJ, 5RED, 5RGR, 5RF9, 5RH4, 5RFD, 5RFB, 5RFC, 7AXM, 5RFV, 5RFW, 5RHB, 6XR3, 6XBG, 6XHM, 5RL2, 7K40, 6WNP, 7D1M, 7K6D, and 7JKV). We used the program SAnDReS [50] to generate this plot. The criteria used to consider intermolecular interactions are the same described for LigPlot+ [52, 53].

we do not have this type of numerical data for any of the structures in the HRM^{pro}. Analysis of HRM^{pro} identified twelve covalent inhibitors and seven crystallization co-factors with no information about the inhibition activity. In Fig. (**1**), we have a map of intermolecular interactions of selected structures generated with SAnDReS. We focused our analysis on inhibitors (covalent and allosteric) and non-covalent ligands bound to the active and alternative sites of M^{pro}.

We can find a detailed description of the three-dimensional structure of M^{pro} elsewhere [68]. Briefly, M^{pro} has the typical structure of 3C-like proteinases found in other coronaviruses. Analysis of its biological unit shows a homodimer. Each M^{pro} monomer has three domains. The first two domains (residues 8-101 and 102-184) show an antiparallel β-barrel structure. The following domain (residues 201–303) contains five α-helices arranged into an antiparallel globular cluster, and it is linked to the second domain by a loop region (residues 185-200). M^{pro} shows a Cys-His catalytic dyad, and the active site is placed between the first two domains [68].

To further investigate intermolecular interactions, we applied the program LigPlot+ to some structures with ligands in HRM^{pro}. Since the binding affinity depends on a wide range of intermolecular interactions [73-80], it is essential to have a standard to determine receptor-ligand contacts. Figs. (**2** and **3**) show the intermolecular interactions of the M^{pro} and selected ligands. Fig. (**2**) shows the ligands for which we have data indicating that the ligand is an inhibitor. Fig. (**3**) shows complexes with non-covalent ligands bound to the active site of M^{pro}, but with no experimental data confirming inhibition.

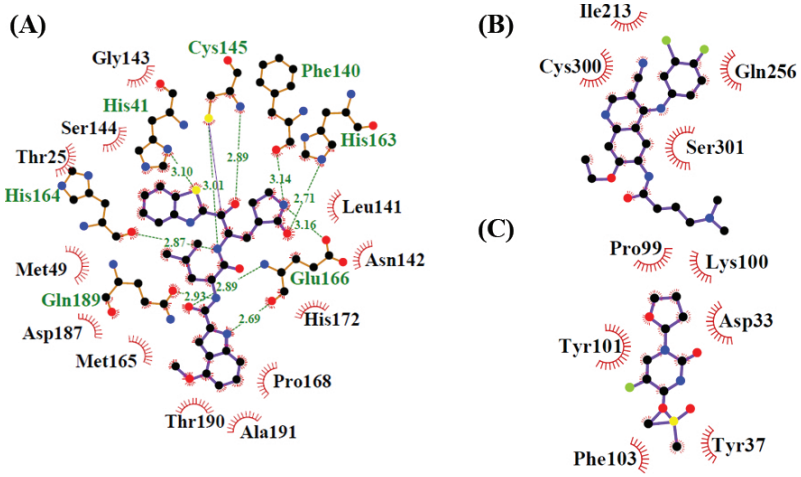

Fig. (2). Intermolecular contacts for inhibitors identified in the structures 7JKV (**A**), 7AXM (**B**), and 7AWR (**C**) using LigPlot+ [52, 53]. These structures have information on the PDB about the inhibition activity of the ligands. In these figures, we present a schematic representation of the residues of M^{pro} participating in Van der Waals contacts and intermolecular hydrogen bonds with ligands. We represent intermolecular hydrogen bonds with dashed lines. The intermolecular distances are in Angstroms. LigPlot+ considers residues as participating in intermolecular hydrogen bonds with the distance between acceptor and donor atoms ranging from 2.8 to 3.4 Å and satisfying the angle criteria [52, 53]. Continuous lines connecting two atoms indicate covalent bonds in the structure. We show the amino acids participating in intermolecular Van der Waals contacts with spiked arcs. We indicate nitrogen atoms in blue, oxygens in red, sulfurs in yellow, halogens in green, and carbons in black. (*A higher resolution / colour version of this figure is available in the electronic copy of the article*).

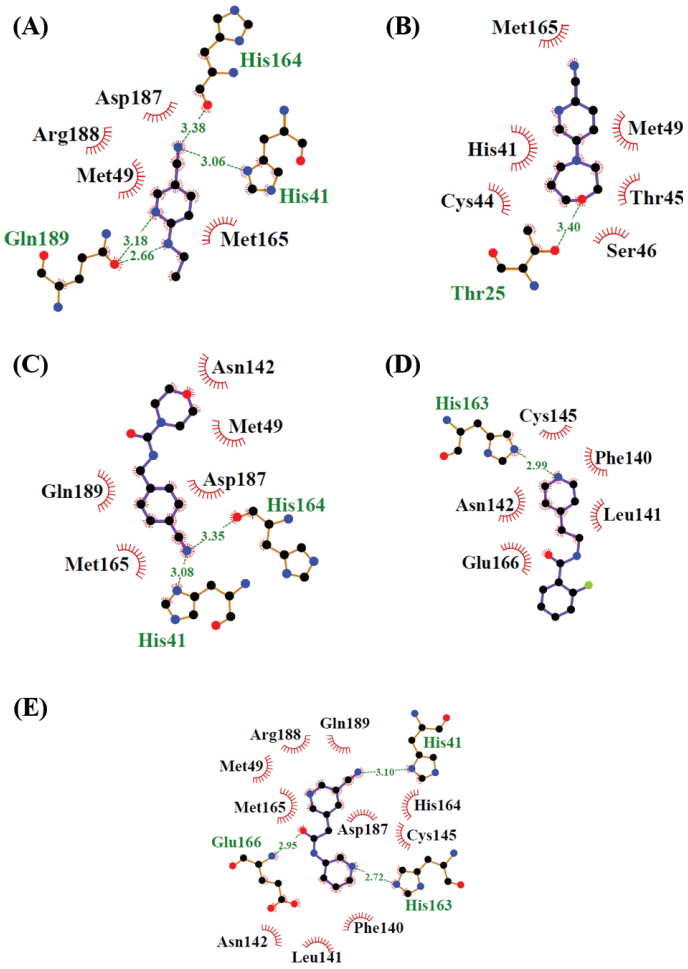

Fig. (3). Intermolecular contacts for non-covalent ligands bound to the active site of M^{pro}. These ligands are present in following the structures: 5R82 (**A**), 5RF6 (**B**), 5RFE (**C**), 5RGK (**D**), and 5RGW (**E**) using LigPlot+ [52, 53]. The definitions used in the legend of Fig. (**2**) also apply here. (*A higher resolution / colour version of this figure is available in the electronic copy of the article*).

Combining the overall view of intermolecular contacts available in Fig. (**1**) and the specific interactions highlighted in Fig. (**2**), we identify three major binding sites. Peaks 1, 2, 3, 5, 6, and 7 in Fig. (**1**) map interactions involving residues in the active site of M^{pro}. The structure described in Fig. (**2A**) indicates the presence of the following residues in the active site of M^{pro}: Thr 25, His 41, Met 49, Phe 140, Leu 141, Asn 142, Gly 143, Ser 144, Cys 145, His 163, His 164, Met 165, Glu 166, Pro 168, His 172, Asp 187, Gln 189, Thr 190, and Ala 191. Cys 145 presents a covalent bond with the inhibitor. Peaks 4 and 8 in Fig. (**1**) indicate intermolecular contacts around residue numbers 100 (Pro 99, Lys 100, Tyr 101, and Phe 103) and 300 (Cys 300 and Ser 301). Analysis of Fig. (**2B**) and Fig. (**2C**) also shows participation residues Asp 33, Tyr 37, Ile 213, and Gln 256 in the allosteric binding sites of M^{pro}. Analysis of intermolecular interactions for structure 7JKV indicates intermolecular hydrogen bonds, Van der Waals interactions, and one covalent bond with the active site. In peaks 4 and 8, we have part of the allosteric binding sites, as seen in structures 7AXM and 7AWR. Analysis of LigPlot+ results for these structures indicated only Van der Waals contacts in the allosteric binding sites.

It is necessary to have experimental data of at least one protein-ligand complex to validate a docking protocol intended to search for potential inhibitors [81-86]. For protein-ligand docking simulations to screen for potential competitive inhibitors of the M^{pro}, the focus should be on the active site. On the other hand, docking screens to find potential allosteric inhibitors should aim at peaks 4 and 8.

We may use the atomic coordinates of any M^{pro} structures highlighted in Fig. (**3**) (PDB access codes:

5R82, 5RF6, 5RFE, 5RGK, and 5RGW) for validation of molecular docking protocols. These complexes have non-covalent ligands bound to the active site, with variation in the interacting residues. Analysis of the intermolecular interactions indicates larger ligands present a higher number of intermolecular contacts. All complexes exhibit intermolecular hydrogen bonds, most with histidine residues, with one exception, *i.e.*, structure 5RF6. In this complex, we have the side chain of Thr 25 participating in a hydrogen bond.

Since there is crystallographic data for M^{pro}, any protein-ligand docking simulations should validate their protocol focusing on these structures. Considering docking simulations using AutoDock4, we have an arsenal of potential docking protocols, combining different search algorithms (LS, SA, GA, and LGA), center of the binding site, and size of the box where the simulation will take place. Also, we could target the AutoDock4 scoring function to the protein system of interest. It is feasible to train the scoring function to predict the binding for a specific protein using machine learning techniques [87-90]. Developing a scoring function specific for a protein system of interest allows us to explore the scoring function space using machine learning methods [34, 50]. These computational approaches increase the chances of finding an adequate computational model to predict protein inhibition [30-33]. In the next section, we discuss selected recent docking studies focused on the active site of M^{pro}.

3.2. Virtual Screening with AutoDock4

AutoDock4 is one of the most successful docking programs used for protein-ligand screening purposes [91]. Due to the large number of AutoDock4 users since the beginning of the COVID-19 pandemic, many research groups started computational screening studies having AutoDock4 as its main docking engine. Search 1 returned eight publications where AutoDock4 was the computational resource for protein-ligand docking simulations [92-99]. These studies used LGA as a search engine with the scoring function defined in equation (**1**). Most of these studies did not report any validation of docking protocols against an experimental complex structure. For docking protocol validation, we need to have at least one crystal structure of the protein with a ligand [100]. High-resolution crystal structures of M^{pro} in complex with inhibitors were available at PDB as early as February 2020 (PDB access code: 6LU7) [101]. Typically, for validation, we report the docking root mean square deviation (RMSD) between the docking pose and the crystallographic position of the ligand [100].

One of the AutoDock4 screening studies reported an RMSD for a cluster of poses, but not against the ligand position in a crystal structure [92]. This approach is a weak validation compared with a docking RMSD against the crystallographic coordinates of a ligand. Also, this study used the structure 6WQF [102] for docking simulations. This structure does not have any ligand bound to the active site, which we should prefer for protein-ligand docking simulations [100]. Other AutoDock4 studies [93-99] took as a target for simulations the crystallographic structure of M^{pro} in complex with N3 peptide inhibitor (PDB access code: 6LU7) [101]. However, the authors did not perform redocking to validate their docking protocol either. Although one AutoDock4 study [98] referenced a redocking simulation with a docking RMSD of 0.254 Å [103], the docking program used in this study [103] is not the AutoDock4, but the related docking program AutoDock Vina [104]. The authors used AutoDock4 for their simulations and justified its application taking as a reference a previously published result that employed a different docking program, which means no validation at all [103].

Adding "deep learning" or "machine learning" to the search (Search 2 and 3) returned zero publications. All AutoDock4 studies relied on equation (**1**) to rank the poses and predict the binding affinity. Considering that we have evidence supporting the application of machine learning methods to develop scoring functions [27-37, 105-110], we expected that some of these computational studies with AutoDock4 would have used machine learning modeling. Unfortunately, none of the AutoDock4 used machine learning approaches. The experimental binding affinity data is available in BindingDB for 150 ligands with IC_{50} data. A dataset large enough to carry out modeling using machine learning approaches in combination with docked poses [111, 112].

Considering AutoDock4 studies related to chloroquine and hydroxychloroquine (Search 4 and 5), we found only one publication [93]. In this study, the authors calculated the binding affinity of chloroquine, hydroxychloroquine, and natural products. We have applications of classical scoring functions to a wide range of protein targets [100]. For proteases, successful application of docking and ranking of poses with classical scoring function identified many HIV-1 protease (EC 3.4.23.16) inhibitors [113, 114]. On the other hand, machine learning methods have an overall predictive performance higher than classical scoring functions, such as the AutoDock4 scoring function [115, 116]. Considering that this study [93] did not apply machine learn-

ing methods to generate a better computational model, it is dangerous to keep these molecules in drug repurposing [117-121] since we have scientific evidence showing that they do not work to treat COVID-19 [16].

The need for drugs to treat COVID-19 is clear, and repurposing is a valid approach in the early stages of drug discovery, where we have the experimental structure of a protein target or at least its homology modeling [91, 122-124]. On the other hand, as we highlighted above, these AutoDock4 studies focused on M^{pro} did not develop machine learning models trained for this protein target. These studies did not report statistical analysis [125] of the predictive performance of scoring functions either. Therefore, the computational prediction of binding affinity for chloroquine and hydroxychloroquine [93] is unreliable. Even worse, this publication [93] gives some grounds for the potential use of these molecules to treat COVID-19.

Many may argue that it is a computational screening, and nobody will take it as scientific proof, but that is not the case. Even with no scientific evidence [16, 126], the Brazilian government distributed chloroquine and hydroxychloroquine to treat COVID-19. Furthermore, since we have scientific data showing these molecules did not work to treat COVID-19 [16], there is no reason to insist on keeping these molecules for drug repurposing studies focused on any protein target of SARS-CoV-2.

3.3. Combining Machine Learning Methods with AutoDock4

As we previously highlighted, so far, all AutoDock4 screens focused on M^{pro} lacked a proper validation of the docking protocol and the predictive performance of the scoring function. These studies also ignored the superior predictive performance of machine learning models compared with classical scoring functions [27-37, 105-110]. Aiming to guide future studies focused on docking screens of potential drugs to treat COVID-19, we propose a combination of molecular simulations (docking and dynamics) and machine learning modeling of scoring functions. We have this integration of computational approaches in one flowchart that may guide future computational studies focused on M^{pro} or any protein target of SARS-CoV-2. Fig. (**4**) shows all steps of this integrated workflow.

Initially, we select a protein target of SARS-CoV-2, for instance, the M^{pro}. In the sequence, we check the availability of experimental data in the PDB. In the absence of structural data for our protein target, we may generate a three-dimensional model based on homology by the satisfaction of spatial restraints implemented in the program MODELER [91, 122-124]. Alternatively, we may use deep learning approaches such as the one implemented in the program AlphaFold [127-129] to generate molecular models for protein where we do not have experimental three-dimensional data. This deep-learning approach recently showed superior predictive performance for structures at CASP (Critical Assessment of protein Structure Prediction) [127, 129].

In the sequence, we check the available binding affinity data at affinity databases such as BindingDB [43, 44], Binding MOAD (Mother of All Databases) [45-47], and PDBbind [48, 49]. For M^{pro}, we have 150 entries at BindingDB with experimental IC_{50} data, a dataset named 3C-like proteinase (SARS-CoV $3C^{pro}$). Following this, we need to validate our AutoDock4 docking protocol. AutoDock4 has four search algorithms available, and we may also vary the grid parameters. Variation of search algorithms and grid parameters may generate different docking results [38, 39].

The best validation for any protein-ligand docking simulation is the ability to reproduce the experimental position of a ligand in the binding pocket of a receptor [100]. For M^{pro}, the experimental result shows a crystal structure of a protein-ligand complex [68]. There are over thirty structures of M^{pro} with a resolution better than 1.5 Å (Table **1**), which is enough experimental data to validate docking protocols. Alternatively, we may consider the binding free energy to select structures to validate docking protocols [37]. This approach has a major issue, *i.e.*, the computational methodology employed to evaluate binding energies. The most reliable methods to address the energetics of protein-ligand interactions make use of quantum mechanics calculation. These methods demand much more computational time when compared with classical approaches [37, 50, 100]. Here, we adopt the criterion of docking RMSD, where we consider satisfactory results, values below 2.0 Å [100].

For the HRM^{pro}, we may choose any structure with a non-covalent ligand for redocking and evaluation of docking RMSD. We can use the remaining data with non-covalent ligands in Table **1** to calculate docking accuracy [100] using the docking protocol that generated the lowest docking RMSD. In the next section, we describe a successful AutoDock4 protocol for M^{pro}. To calculate docking accuracy (DA), we may use the following equation:

$$DA = f_l + 0.5(f_l - f_h) \quad (3)$$

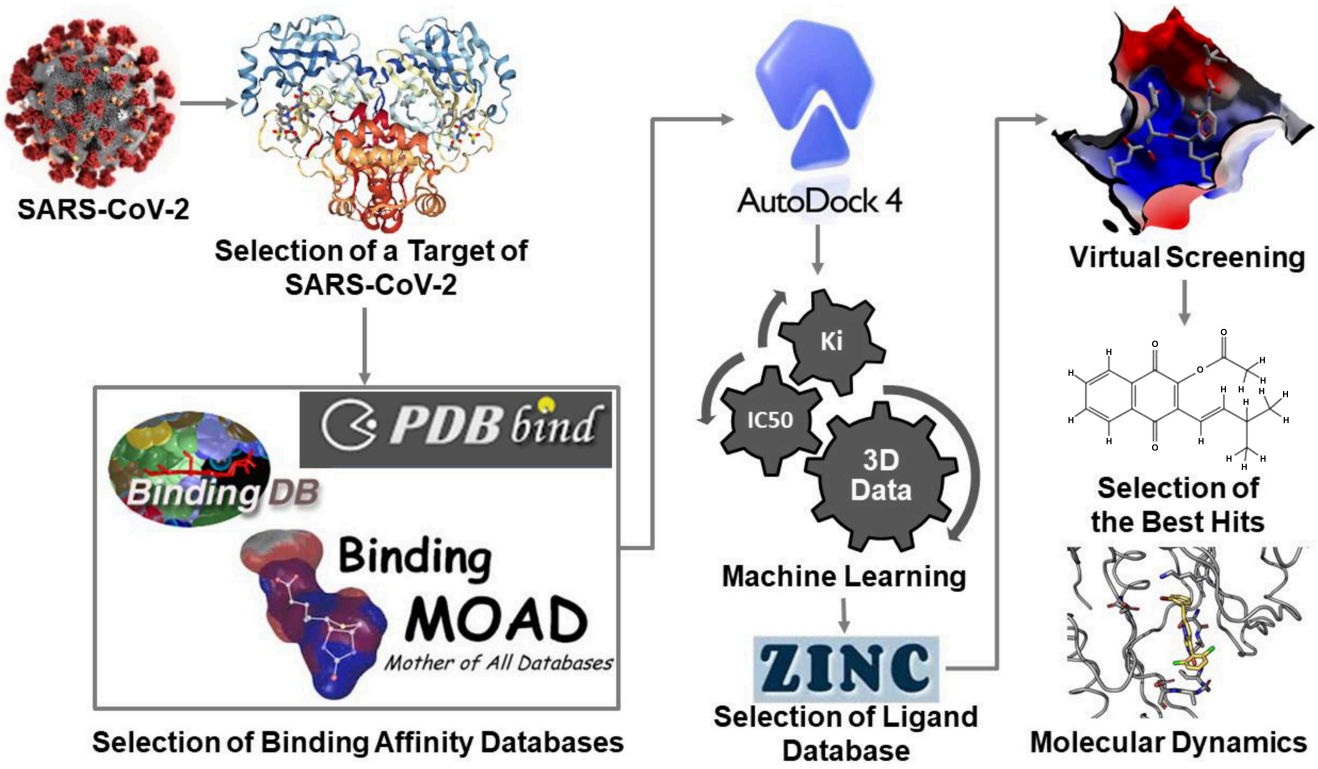

Fig. (4). Schematic flowchart showing a workflow to combine protein-ligand docking simulations with AutoDock4, machine learning modeling, and molecular dynamics simulations. Initially, we select a protein target for which atomic coordinates are available. Then, we gather binding affinity data found in databases such as BindingDB [43, 44], Binding MOAD [45-47], and PDBbind [48, 49]. After that, we carry out docking simulations to validate a docking protocol using previously selected atomic coordinates of the protein target. Next, we employ this docking protocol to dock ligands found in the binding databases to the structure of our protein target. In this phase, we generate the raw material for the machine learning modeling. In the machine learning phase, we generate a scoring function trained using the structures we obtained through docking simulations. Then, we choose potential ligands from the ZINC database [138-140]. Following that, we submit the potential ligands chosen from the ZINC for virtual screening. In this phase, we apply the validated docking protocol against the atomic coordinates of the protein target. We select the best hits using the machine-learning scoring function. After selection of the best hits, we submit the structures of these complexes (protein and best hits) to molecular dynamics simulations. We expect to assess the structural stability of the protein-ligand complexes during this phase. (*A higher resolution / colour version of this figure is available in the electronic copy of the article*).

Where f_l represents the fraction poses for which the docking RMSD is less than l, and f_h indicates the fraction of poses for which the docking RMSD is less than h, where $l < h$ [100]. In equation (**3**), the typical values of l and h are 2.0 and 3.0 Å, respectively. We expect values of DA > 0.6 for successful docking protocols [50].

Following this, we execute the machine-learning phase, where we apply the validated docking protocol to generate protein-ligand complexes for the ligands for which we have binding affinity data. In the case of M^{pro}, we have 150 ligands with IC_{50} data at BindingDB. We may use as a target the structure 5RGW. Considering recent machine learning approaches to calculate binding affinity or thermodynamic data (ΔG) from the atomic coordinates of receptor-ligand complexes, we may use any of the following machine learning programs: Molegro Data Modeller [130-132], Pafnucy [133], property-encoded shape distributions together with standard support vector machine (PESD-SVM) [134], Neural-Network-Based Scoring function (NNScore series) [135-137], Random Forest Score (RF-Score series) [27, 28], Statistical Analysis of Docking Results and Scoring Functions (SAnDReS) [50], and Tool to Analyze the Binding Affinity (Taba) [31, 32].

In the sequence, we use the best machine learning model selected using the predictive performance [32]

and choose a subset of potential binders available in a ligand database such as ZINC [138-140]. Finally, we choose the best hits with the lowest value of the machine-learning scoring function and submit them to molecular dynamics simulations. Among the previously AutoDock4 published studies [92-99], two works also employed molecular dynamics simulations (Search 6) [96, 97]. We use molecular dynamics simulations to confirm the binding of ligands [141-145]. We may also investigate the dynamics of protein-ligand interactions [145].

In summary, this workflow combines established computational methodologies such as protein-ligand docking and molecular dynamics simulations with state-of-art approaches involving the application of machine learning methods to generate targeted-scoring functions. In doing so, we make available an integrated methodology that has a system-level approach to the problem of drug discovery. We previously applied this integrated approach to study other protein targets [110].

Such a combination of computational tools explores the scoring function space [105]. This mathematical space is the result of the relationship involving the chemical and the protein spaces. In this approach, we select an element of the protein space, for instance, M^{pro}. We identify a subspace of the chemical space composed of inhibitors of the M^{pro}. Using machine learning methods, we explore the scoring function space. As a result, we find an adequate model trained to predict binding affinity. This scoring function employs the atomic coordinates of protein-ligand complexes as input and calculates the binding affinity. This model is an equation determined by methods of machine learning implemented in programs such as Taba [31] and SAnDReS [50].

Here, we gave an overview of how to integrate different computational methods for projects of drug discovery. Scientifically, our goal is to review published works focused on the application of AutoDock4 to the study of potential inhibitors of M^{pro}. We did not intend to cover the development of machine learning models, molecular docking, and dynamics simulations of M^{pro}. We explain the details of applying machine learning methods to generate targeted-scoring functions elsewhere [31, 50]. We may find an updated description of how to carry out molecular dynamics simulations of protein-ligand complexes in recent publications [141, 144]. Since most of the previously AutoDock4 applications [92-99] did not give details about their docking protocols, in the following section, we describe a docking protocol using AutoDock4 for M^{pro}.

3.4. Validation of AutoDock4 Protocol for M^{pro}

Although we have eight previously published AutoDock4 studies [92-99] focused on M^{pro}, most of them did not validate their computational approaches for protein-ligand docking simulations. The majority of the published docking studies using AutoDock4 did not mention details about their docking protocols, such as the center of the binding site and the size of the box where the simulation took place. To facilitate further protein-ligand docking studies focused on M^{pro}, we give below full details of our proposed docking protocol using AutoDock4 using a crystal structure with a resolution better than 1.5 Å.

Considering the structures in the HRM^{pro}, we may use the crystal structure 5RGW (solved at 1.43 Å) determined to a better resolution compared to 6LU7 [101] (solved at 2.16 Å resolution). For docking simulations against this structure, we used default parameters of LGA [38, 39] as a search algorithm for the ligand UGM (2-(5-cyanopyridin-3-yl)-N-(pyridin-3-yl) acetamide) without water molecules and co-factors. We separated the original PDB file into two PDB files, one for the ligand (UGM) and the second for the protein. We converted them to PDBQT format using SAnDReS [50]. Charges for ligand and protein atoms were assigned using the Gasteiger-Marsili method [146-148] implemented in the program AutoDockTools4 [38]. The grid for docking simulations had as center coordinates 10.034, -0.723, and 20.955 Å, with a box of 11.25, 9.0, and 6.75 Å, and spacing of 0.375 Å. This grid box encompasses the active site of M^{pro} and the ligand. Fig. (**5**) shows the lowest energy pose.

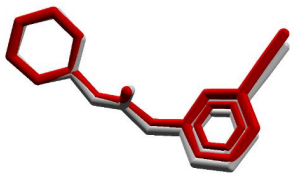

Fig. (5). Lowest energy pose generated using AutoDock4 for the ligand UGM of the structure 5RGW. Ligand in light gray indicates the crystallographic position and red the pose. We used the program Molegro Virtual Docker [130] to generate this figure. (*A higher resolution / colour version of this figure is available in the electronic copy of the article*).

After docking simulation, the lowest energy pose presents a docking RMSD of 0.47 Å. This pose has binding energy calculated using equation (**1**) of -7.78 kcal/mol. This result strongly indicates that this docking protocol is adequate for virtual screening studies.

Table 2. Summary of docking protocols using AutoDock 4 for M^{pro}.

PDB	Resolution (Å)	Ligand	Grid (grid points)	Grid Center (Å)	Spacing (Å)	RMSD (Å)	References
6Y2F	1.95	O6K	55 × 55 × 54	11.207, -1.020, 20.757	0.375	NR	[172]
6LU7	2.16	N3	60 x 60 x 60	-9.732, 11.403, 68.925	0.375	1.9	[173]
6LU7	2.16	N3	50 x 50 x 50	-9.100, 11.000, 68.000	0.375	NR	[174]
6LU7	2.16	N3	58 x 68 x 70	-10.883, 13.934, 68.209	0.375	1.47	[175]
6M03	2.00	None	60 x 60 x 60	NR	0.375	Apo form	[176]
5RGW	1.43	UGM	30 x 24 x 18	10.034, -0.723, 20.955	0.375	0.47	This work

NR: Not reported by the authors.

3.5. Additional Docking Studies for M^{pro}

Our goal here is to review the efforts to identify inhibitors of the M^{pro} using the program AutoDock4. We also would like to mention few docking simulation studies using the following programs: AutoDock Vina [149-158], SwissDock [159], Molegro Virtual Docker [160-162], and others [163-169]. All these simulations relied on structures available for M^{pro} in complex with ligands. These studies identified inhibitors bound to the active site with relatively low estimated binding scores [149-169], which might contribute to the identification of a potential new drug to treat COVID-19. It has been found that the sites, as well as the number and length of mature peptides cleaved by the 3C-like proteinase, are highly conserved among different groups of coronaviruses [170], including SARS-CoV-2 [171].

Besides the previously mentioned eight studies using AutoDock4 [92-99] employed to identify potential inhibitors of M^{pro}, during the reviewing process of this paper, additional works were published [172-176]. We show these docking protocols in Table **2**. Most of these docking studies focused on the structure 6LU7 [173-175], ignoring available higher-resolution crystallographic structures (Table **1**). These new works reported, at least partially, their docking protocols. However, most of them did not validate their computational approach reporting the docking RMSD. For those reporting docking RMSD, they have values higher than 1.4 Å. For all docking simulations, the authors used the LGA as a search engine in their docking simulations. AutoDock4 has a total of four docking search engines, but due to the docking accuracy and faster algorithm, most of the recent studies using AutoDock4 employed LGA [39]. Among the docking protocols using AutoDock4 (Table **2**), our approach uses the highest crystallographic resolution structure and presents the lowest docking RMSD.

CONCLUSION

In this review, we described recent applications of protein-ligand docking simulations focused on the M^{pro} using AutoDock4. All these drug screenings relied on the newly deposited crystallographic structures of this enzyme. Most of these studies used atomic coordinates of entry 6LU7. Such works revealed a concentrated effort to contribute to a possible cure for COVID-19. On the other hand, the urgency to find a cure for COVID-19 does not justify the careless use of docking simulations. We reviewed eight works published in peer-reviewed journals, and these studies ignored the use of recent technologies, such as the application of machine learning. We highlighted the danger of using chloroquine and hydroxychloroquine in a dataset for drug repurposing. These molecules have no positive effect as drugs to treat COVID-19. Insisting on their use to treat COVID-19 is a denial of science. We expect to contribute to future works with a validated docking protocol using AutoDock4 for M^{pro}, as far as we know, the first to employ a crystal structure solved to a resolution better than 1.5 Å. Also, we suggested a workflow integrating machine learning with molecular simulations to improve the predictive performance of future docking screens focused on M^{pro}.

LIST OF ABBREVIATIONS

CASP	=	Critical Assessment of Protein Structure Prediction
COVID-19	=	Coronavirus Disease of 2019
ΔG	=	Variation of Gibbs Free Energy of Binding
EC	=	Enzyme Classification Number
GA	=	Genetic Algorithm
HRM^{pro}	=	High-resolution Main Protease of SARS-CoV-2 Dataset

IC_{50}	= Half-maximal Inhibitory Concentration
K_d	= Dissociation Constant
K_i	= Inhibition Constant
LGA	= Lamarckian Genetic Algorithm
LS	= Local Search
MOAD	= Mother of All Databases
M^{pro}	= Main Protease of SARS-CoV-2
PEOE	= Partial Equalization of Orbital Electronegativity
PDB	= Protein Data Bank
RMSD	= Root Mean Square Deviation
SA	= Simulated Annealing
SAnDReS	= Statistical Analysis of Docking Results and Scoring Functions
SARS-CoV-2	= Severe Acute Respiratory Syndrome Coronavirus 2
SBDD	= Structure-based Drug Design
Taba	= Tool to Analyze the Binding Affinity

CONSENT FOR PUBLICATION

Not applicable.

FUNDING

This study has been financed in part by the Coordenação de Aperfeiçoamento de Pessoal de Nível Superior - Brasil (CAPES) - Finance Code 001.

Walter Filgueira de Azevedo Junior is a researcher for CNPq, Brazil (Process Numbers: 308883/2014-4 and 309029/2018-0).

CONFLICT OF INTEREST

The authors declare no conflict of interest, financial or otherwise.

ACKNOWLEDGEMENTS

Joana Retzke Godoy acknowledges the CNPq undergraduate fellowship, Brazil.

The authors acknowledge the assistance of the reviewers of this work, who helped them in many ways through their enlightening comments and valuable suggestions. Without their contributions, this manuscript would not be possible.

REFERENCES

[1] Borah, P.; Deb, P.K.; Deka, S.; Venugopala, K.N.; Singh, V.; Mailavaram, R.P.; Kalia, K.; Tekade, R.K. Current scenario and future prospect in the management of COVID-19. *Curr. Med. Chem.,* **2021**, *28*(2), 284-307. http://dx.doi.org/10.2174/0929867327666200908113642 PMID: 32900341

[2] Kumar, R.; Harilal, S.; Al-Sehemi, A.G.; Mathew, G.E.; Carradori, S.; Mathew, B. The chronicle of COVID-19: possible strategies to curb the pandemic. *Curr. Med. Chem.,* **2021**, *28*(15), 2852-2886. http://dx.doi.org/10.2174/0929867327666200702151018 PMID: 32614740

[3] Sharma, A.K.; Sharma, V.; Sharma, A.; Pallikkuth, S.; Sharma, A.K. Current paradigms in COVID-19 research: proposed treatment strategies, recent trends and future directions. *Curr. Med. Chem.,* **2021**, *28*(16), 3173-3192. http://dx.doi.org/10.2174/0929867327666200711153829 PMID: 32651959

[4] de Barcelos Ubaldo Martins, L.; Jabour, L.G.P.P.; Vieira, C.C.; Nery, L.C.C.; Dias, R.F.; Simões E Silva, A.C. Renin-angiotensin system (RAS) and immune system profile in specific subgroups with COVID-19. *Curr. Med. Chem.,* **2021**, *28*(22), 4499-4530. http://dx.doi.org/10.2174/0929867327666200903113117 PMID: 32881654

[5] Pena, A.L.B.; Oliveira, R.A.; Severo, R.G.; Simões E Silva, A.C. COVID-19 related coagulopathy: what is known up to now. *Curr. Med. Chem.,* **2021**, *28*(21), 4207-4225. http://dx.doi.org/10.2174/0929867327666201005112231 PMID: 33019920

[6] Priyadarshini, I.; Mohanty, P.; Kumar, R.; Son, L.H.; Chau, H.T.M.; Nhu, V.H.; Thi Ngo, P.T.; Tien Bui, D. Analysis of outbreak and global impacts of the COVID-19. *Healthcare (Basel),* **2020**, *8*(2), 148. http://dx.doi.org/10.3390/healthcare8020148 PMID: 32485875

[7] Dong, E.; Du, H.; Gardner, L. An interactive web-based dashboard to track COVID-19 in real time. *Lancet Infect. Dis.,* **2020**, *20*(5), 533-534. http://dx.doi.org/10.1016/S1473-3099(20)30120-1 PMID: 32087114

[8] Cimerman, S.; Chebabo, A.; Cunha, C.A.D.; Rodríguez-Morales, A.J. Deep impact of COVID-19 in the healthcare of Latin America: the case of Brazil. *Braz. J. Infect. Dis.,* **2020**, *24*(2), 93-95. http://dx.doi.org/10.1016/j.bjid.2020.04.005 PMID: 32335078

[9] Aquino, E.M.L.; Silveira, I.H.; Pescarini, J.M.; Aquino, R.; Souza-Filho, J.A.; Rocha, A.S.; Ferreira, A.; Victor, A.; Teixeira, C.; Machado, D.B.; Paixão, E.; Alves, F.J.O.; Pilecco, F.; Menezes, G.; Gabrielli, L.; Leite, L.; Almeida, M.C.C.; Ortelan, N.; Fernandes, Q.H.R.F.; Ortiz, R.J.F.; Palmeira, R.N.; Junior, E.P.P.; Aragão, E.; Souza, L.E.P.F.; Netto, M.B.; Teixeira, M.G.; Barreto, M.L.; Ichihara, M.Y.; Lima, R.T.R.S. Social distancing measures to control the COVID-19 pandemic: potential impacts and challenges in Brazil. *Cien. Saude Colet.,* **2020**, *25*(Suppl. 1), 2423-2446. http://dx.doi.org/10.1590/1413-81232020256.1.10502020 PMID: 32520287

[10] Sen-Crowe, B.; McKenney, M.; Elkbuli, A. Social distancing during the COVID-19 pandemic: staying home save lives. *Am. J. Emerg. Med.,* **2020**, *38*(7), 1519-1520.

http://dx.doi.org/10.1016/j.ajem.2020.03.063 PMID: 32305155

[11] Idrovo, A.J.; Manrique-Hernández, E.F.; Fernández Niño, J.A. Report from Bolsonaro's Brazil: the consequences of ignoring science. *Int. J. Health Serv.,* **2021**, *51*(1), 31-36. http://dx.doi.org/10.1177/0020731420968446 PMID: 33100167

[12] Falkenbach, M.; Greer, S.L. Denial and distraction: how the populist radical right responds to COVID-19 comment on "a scoping review of prr parties' influence on welfare policy and its implication for population healthin Europe". *Int. J. Health Policy Manag.,* **2020**. Epub Ahead of Print http://dx.doi.org/10.34172/ijhpm.2020.141 PMID: 32772011

[13] Carnut, L.; Mendes, Á.; Guerra, L. Coronavirus, capitalism in crisis and the perversity of public health in Bolsonaro's Brazil. *Int. J. Health Serv.,* **2020**, *51*(1), 18-30. http://dx.doi.org/10.1177/0020731420965137 PMID: 33070682

[14] Ortega, F.; Orsini, M. Governing COVID-19 without government in Brazil: ignorance, neoliberal authoritarianism, and the collapse of public health leadership. *Glob. Public Health,* **2020**, *15*(9), 1257-1277. http://dx.doi.org/10.1080/17441692.2020.1795223 PMID: 32663117

[15] Shrestha, N.; Shad, M.Y.; Ulvi, O.; Khan, M.H.; Karamehic-Muratovic, A.; Nguyen, U.D.T.; Baghbanzadeh, M.; Wardrup, R.; Aghamohammadi, N.; Cervantes, D.; Nahiduzzaman, K.M.; Zaki, R.A.; Haque, U. The impact of COVID-19 on globalization. *One Health,* **2020**, *11*, 100180. http://dx.doi.org/10.1016/j.onehlt.2020.100180 PMID: 33072836

[16] Hoffmann, M.; Mösbauer, K.; Hofmann-Winkler, H.; Kaul, A.; Kleine-Weber, H.; Krüger, N.; Gassen, N.C.; Müller, M.A.; Drosten, C.; Pöhlmann, S. Chloroquine does not inhibit infection of human lung cells with SARS-CoV-2. *Nature,* **2020**, *585*(7826), 588-590. http://dx.doi.org/10.1038/s41586-020-2575-3 PMID: 32698190

[17] Campillo, N.E.; Jimenez, M.; Canelles, M. COVID-19 vaccine race: analysis of age-dependent immune responses against SARS-CoV-2 indicates that more than just one strategy may be needed. *Curr. Med. Chem.,* **2021**, *28*(20), 3964-3979. http://dx.doi.org/10.2174/0929867327666201027153123 PMID: 33109026

[18] Nascimento, I.J.D.S; de Aquino, T.M.; da Silva-Júnior, E.F. Drug repurposing: a strategy for discovering inhibitors against emerging viral infections. *Curr. Med. Chem.,* **2021**, *28*(15), 2887-2942. http://dx.doi.org/10.2174/0929867327666200812215852 PMID: 32787752

[19] Luan, B.; Huynh, T.; Cheng, X.; Lan, G.; Wang, H.-R. Targeting proteases for treating COVID-19. *J. Proteome Res.,* **2020**, *19*(11), 4316-4326. http://dx.doi.org/10.1021/acs.jproteome.0c00430 PMID: 33090793

[20] Li, J.; Zhou, X.; Zhang, Y.; Zhong, F.; Lin, C.; McCormick, P.J.; Jiang, F.; Luo, J.; Zhou, H.; Wang, Q.; Fu, Y.; Duan, J.; Zhang, J. Crystal structure of SARS-CoV-2 main protease in complex with the natural product inhibitor shikonin illuminates a unique binding mode. *Sci. Bull. (Beijing),* **2021**, *66*(7), 661-663. http://dx.doi.org/10.1016/j.scib.2020.10.018 PMID: 33163253

[21] Zhang, L.; Lin, D.; Sun, X.; Curth, U.; Drosten, C.; Sauerhering, L.; Becker, S.; Rox, K.; Hilgenfeld, R. Crystal structure of SARS-CoV-2 main protease provides a basis for design of improved α-ketoamide inhibitors. *Science,* **2020**, *368*(6489), 409-412. http://dx.doi.org/10.1126/science.abb3405 PMID: 32198291

[22] Mengist, H.M.; Fan, X.; Jin, T. Designing of improved drugs for COVID-19: crystal structure of SARS-CoV-2 main protease M^{pro}. *Signal Transduct. Target. Ther.,* **2020**, *5*(1), 67. http://dx.doi.org/10.1038/s41392-020-0178-y PMID: 32388537

[23] Bockman, M.R.; Mishra, N.; Aldrich, C.C. The biotin biosynthetic pathway in *Mycobacterium tuberculosis* is a validated target for the development of antibacterial agents. *Curr. Med. Chem.,* **2020**, *27*(25), 4194-4232. http://dx.doi.org/10.2174/0929867326666190119161551 PMID: 30663561

[24] Xia, J.; Feng, B.; Wen, G.; Xue, W.; Ma, G.; Zhang, H.; Wu, S. Bacterial lipoprotein biosynthetic pathway as a potential target for structure-based design of antibacterial agents. *Curr. Med. Chem.,* **2020**, *27*(7), 1132-1150. http://dx.doi.org/10.2174/0929867325666181008143411 PMID: 30360704

[25] Xue, W.; Fu, T.; Zheng, G.; Tu, G.; Zhang, Y.; Yang, F.; Tao, L.; Yao, L.; Zhu, F. Recent advances and challenges of the drugs acting on monoamine transporters. *Curr. Med. Chem.,* **2020**, *27*(23), 3830-3876. http://dx.doi.org/10.2174/0929867325666181009123218 PMID: 30306851

[26] Lawal, M.M.; Sanusi, Z.K.; Govender, T.; Maguire, G.E.M.; Honarparvar, B.; Kruger, H.G. From recognition to reaction mechanism: an overview on the interactions between HIV-1 protease and its natural targets. *Curr. Med. Chem.,* **2020**, *27*(15), 2514-2549. http://dx.doi.org/10.2174/0929867325666181113122900 PMID: 30421668

[27] Ballester, P.J.; Mitchell, J.B.O. A machine learning approach to predicting protein-ligand binding affinity with applications to molecular docking. *Bioinformatics,* **2010**, *26*(9), 1169-1175. http://dx.doi.org/10.1093/bioinformatics/btq112 PMID: 20236947

[28] Ballester, P.J.; Schreyer, A.; Blundell, T.L. Does a more precise chemical description of protein-ligand complexes lead to more accurate prediction of binding affinity? *J. Chem. Inf. Model.,* **2014**, *54*(3), 944-955. http://dx.doi.org/10.1021/ci500091r PMID: 24528282

[29] Li, H.; Leung, K.S.; Ballester, P.J.; Wong, M.H. istar: a web platform for large-scale protein-ligand docking. *PLoS One,* **2014**, *9*(1), e85678. http://dx.doi.org/10.1371/journal.pone.0085678 PMID: 24475049

[30] Wójcikowski, M.; Siedlecki, P.; Ballester, P.J. Building machine-learning scoring functions for structure-based prediction of intermolecular binding affinity. *Methods Mol. Biol.,* **2019**, *2053*, 1-12. http://dx.doi.org/10.1007/978-1-4939-9752-7_1 PMID: 31452095

[31] da Silva, A.D.; Bitencourt-Ferreira, G.; de Azevedo, W.F.Jr. Taba: a tool to analyze the binding affinity. *J. Comput. Chem.,* **2020**, *41*(1), 69-73. http://dx.doi.org/10.1002/jcc.26048 PMID: 31410856

[32] Bitencourt-Ferreira, G.; da Silva, A.D.; de Azevedo, W.F.Jr. Application of machine learning techniques to predict binding affinity for drug targets. A study of cyclin-dependent kinase 2. *Curr. Med. Chem.,* **2021**, *28*(3), 253-265. http://dx.doi.org/10.2174/2213275912666191102162959 PMID: 31729287

[33] Bitencourt-Ferreira, G.; Rizzotto, C.; de Azevedo, W.F.Jr. Machine learning-based scoring functions, development and applications with SAnDReS. *Curr. Med. Chem.,* **2021**, *28*(9), 1746-1756. http://dx.doi.org/10.2174/0929867327666200515101820 PMID: 32410551

[34] de Ávila, M.B.; Xavier, M.M.; Pintro, V.O.; de Azevedo, W.F. Jr. Supervised machine learning techniques to predict binding affinity. A study for cyclin-dependent kinase 2. *Biochem. Biophys. Res. Commun.,* **2017**, *494*(1-2), 305-310. http://dx.doi.org/10.1016/j.bbrc.2017.10.035 PMID: 29017921

[35] Levin, N.M.B.; Pintro, V.O.; Bitencourt-Ferreira, G.; de Mattos, B.B.; de Castro Silvério, A.; de Azevedo, W.F. Jr. Development of CDK-targeted scoring functions for prediction of binding affinity. *Biophys. Chem.,* **2018**, *235*, 1-8. http://dx.doi.org/10.1016/j.bpc.2018.01.004 PMID: 29407904

[36] de Ávila, M.B.; de Azevedo, W.F. Jr. Development of machine learning models to predict inhibition of 3-dehydroquinate dehydratase. *Chem. Biol. Drug Des.,* **2018**, *92*(2), 1468-1474. http://dx.doi.org/10.1111/cbdd.13312 PMID: 29676519

[37] Bitencourt-Ferreira, G.; de Azevedo, W.F. Jr. Development of a machine-learning model to predict Gibbs free energy of binding for protein-ligand complexes. *Biophys. Chem.,* **2018**, *240*, 63-69. http://dx.doi.org/10.1016/j.bpc.2018.05.010 PMID: 29906639

[38] Morris, G.M.; Huey, R.; Lindstrom, W.; Sanner, M.F.; Belew, R.K.; Goodsell, D.S.; Olson, A.J. AutoDock4 and AutoDockTools4: automated docking with selective receptor flexibility. *J. Comput. Chem.,* **2009**, *30*(16), 2785-2791. http://dx.doi.org/10.1002/jcc.21256 PMID: 19399780

[39] Bitencourt-Ferreira, G.; Pintro, V.O.; de Azevedo, W.F. Jr. Docking with AutoDock4. *Methods Mol. Biol.,* **2019**, *2053*, 125-148. http://dx.doi.org/10.1007/978-1-4939-9752-7_9 PMID: 31452103

[40] Berman, H.M.; Westbrook, J.; Feng, Z.; Gilliland, G.; Bhat, T.N.; Weissig, H.; Shindyalov, I.N.; Bourne, P.E. The protein data bank. *Nucleic Acids Res.,* **2000**, *28*(1), 235-242. http://dx.doi.org/10.1093/nar/28.1.235 PMID: 10592235

[41] Berman, H.M.; Battistuz, T.; Bhat, T.N.; Bluhm, W.F.; Bourne, P.E.; Burkhardt, K.; Feng, Z.; Gilliland, G.L.; Iype, L.; Jain, S.; Fagan, P.; Marvin, J.; Padilla, D.; Ravichandran, V.; Schneider, B.; Thanki, N.; Weissig, H.; Westbrook, J.D.; Zardecki, C. The protein data bank. *Acta Crystallogr. D Biol. Crystallogr,* **2002**, *58*(Pt 6 No 1), 899-907. http://dx.doi.org/10.1107/S0907444902003451 PMID: 12037327

[42] Westbrook, J.; Feng, Z.; Chen, L.; Yang, H.; Berman, H.M. The protein data bank and structural genomics. *Nucleic Acids Res.,* **2003**, *31*(1), 489-491. http://dx.doi.org/10.1093/nar/gkg068 PMID: 12520059

[43] Liu, T.; Lin, Y.; Wen, X.; Jorissen, R.N.; Gilson, M.K. BindingDB: a web-accessible database of experimentally determined protein-ligand binding affinities. *Nucleic Acids Res.,* **2007**, *35*(Database issue), D198-D201. http://dx.doi.org/10.1093/nar/gkl999 PMID: 17145705

[44] Gilson, M.K.; Liu, T.; Baitaluk, M.; Nicola, G.; Hwang, L.; Chong, J. BindingDB in 2015: a public database for medicinal chemistry, computational chemistry and systems pharmacology. *Nucleic Acids Res.,* **2016**, *44*(D1), D1045-D1053. http://dx.doi.org/10.1093/nar/gkv1072 PMID: 26481362

[45] Smith, R.D.; Clark, J.J.; Ahmed, A.; Orban, Z.J.; Dunbar, J.B.Jr. ; Carlson, H.A. Updates to binding MOAD (mother of all databases): polypharmacology tools and their utility in drug repurposing. *J. Mol. Biol.,* **2019**, *431*(13), 2423-2433. http://dx.doi.org/10.1016/j.jmb.2019.05.024 PMID: 31125569

[46] Benson, M.L.; Smith, R.D.; Khazanov, N.A.; Dimcheff, B.; Beaver, J.; Dresslar, P.; Nerothin, J.; Carlson, H.A. Binding MOAD, a high-quality protein-ligand database. *Nucleic Acids Res.,* **2008**, *36*(Database issue), D674-D678. PMID: 18055497

[47] Ahmed, A.; Smith, R.D.; Clark, J.J.; Dunbar, J.B.Jr.; Carlson, H.A. Recent improvements to binding MOAD: a resource for protein-ligand binding affinities and structures. *Nucleic Acids Res.,* **2015**, *43*(Database issue), D465-D469. http://dx.doi.org/10.1093/nar/gku1088 PMID: 25378330

[48] Liu, Z.; Li, Y.; Han, L.; Li, J.; Liu, J.; Zhao, Z.; Nie, W.; Liu, Y.; Wang, R. PDB-wide collection of binding data: current status of the PDBbind database. *Bioinformatics,* **2015**, *31*(3), 405-412. http://dx.doi.org/10.1093/bioinformatics/btu626 PMID: 25301850

[49] Liu, Z.; Li, J.; Liu, J.; Liu, Y.; Nie, W.; Han, L.; Li, Y.; Wang, R. Cross-Mapping of protein-ligand binding data between ChEMBL and PDBbind. *Mol. Inform.,* **2015**, *34*(8), 568-576. http://dx.doi.org/10.1002/minf.201500010 PMID: 27490502

[50] Xavier, M.M.; Heck, G.S.; Avila, M.B.; Levin, N.M.B.; Pintro, V.O.; Carvalho, N.L.; Azevedo, W.F. Jr. SAnDReS a computational tool for statistical analysis of docking results and development of scoring functions. *Comb. Chem. High Throughput Screen.,* **2016**, *19*(10), 801-812. http://dx.doi.org/10.2174/1386207319666160927111347 PMID: 27686428

[51] Bitencourt-Ferreira, G.; de Azevedo, W.F. Jr. SAnDReS: A computational tool for docking. *Methods Mol. Biol.,* **2019**, *2053*, 51-65. http://dx.doi.org/10.1007/978-1-4939-9752-7_4 PMID: 31452098

[52] Wallace, A.C.; Laskowski, R.A.; Thornton, J.M. LIGPLOT: a program to generate schematic diagrams of protein-ligand interactions. *Protein Eng.,* **1995**, *8*(2), 127-134. http://dx.doi.org/10.1093/protein/8.2.127 PMID: 7630882

[53] Laskowski, R.A.; Swindells, M.B. LigPlot+: multiple ligand-protein interaction diagrams for drug discovery. *J. Chem. Inf. Model.,* **2011**, *51*(10), 2778-2786. http://dx.doi.org/10.1021/ci200227u PMID: 21919503

[54] Lipinski, C.A.; Lombardo, F.; Dominy, B.W.; Feeney, P.J. Experimental and computational approaches to estimate solubility and permeability in drug discovery and development settings. *Adv. Drug Deliv. Rev.,* **2001**, *46*(1-3), 3-26.

http://dx.doi.org/10.1016/S0169-409X(00)00129-0 PMID: 11259830

[55] Lennard-Jones, J.E. Cohesion. *Proc. Phys. Soc.,* **1931**, *43*(5), 461. http://dx.doi.org/10.1088/0959-5309/43/5/301

[56] Cornell, W.D.; Cieplak, P.; Bayly, C.I.; Gould, I.R.; Merz, K.M.; Ferguson, D.M.; Spellmeyer, D.C.; Fox, T.; Caldwell, J.W.; Kollman, P.A. A second generation force field for the simulation of proteins, nucleic acids, and organic molecules. *J. Am. Chem. Soc.,* **1995**, *117*, 5179-5197. http://dx.doi.org/10.1021/ja00124a002

[57] Hornak, V.; Abel, R.; Okur, A.; Strockbine, B.; Roitberg, A.; Simmerling, C. Comparison of multiple amber force fields and development of improved protein backbone parameters. *Proteins,* **2006**, *65*(3), 712-725. http://dx.doi.org/10.1002/prot.21123 PMID: 16981200

[58] Mehler, E.L.; Solmajer, T. Electrostatic effects in proteins: comparison of dielectric and charge models. *Protein Eng.,* **1991**, *4*(8), 903-910. http://dx.doi.org/10.1093/protein/4.8.903 PMID: 1667878

[59] Li, L.; Li, C.; Zhang, Z.; Alexov, E. On the dielectric "constant" of proteins: smooth dielectric function for macromolecular modeling and its implementation in DelPhi. *J. Chem. Theory Comput.,* **2013**, *9*(4), 2126-2136. http://dx.doi.org/10.1021/ct400065j PMID: 23585741

[60] Kato, M.; Pisliakov, A.V.; Warshel, A. The barrier for proton transport in aquaporins as a challenge for electrostatic models: the role of protein relaxation in mutational calculations. *Proteins,* **2006**, *64*(4), 829-844. http://dx.doi.org/10.1002/prot.21012 PMID: 16779836

[61] Gouda, H.; Kuntz, I.D.; Case, D.A.; Kollman, P.A. Free energy calculations for theophylline binding to an RNA aptamer: comparison of MM-PBSA and thermodynamic integration methods. *Biopolymers,* **2003**, *68*(1), 16-34. http://dx.doi.org/10.1002/bip.10270 PMID: 12579577

[62] Kollman, P.A.; Massova, I.; Reyes, C.; Kuhn, B.; Huo, S.; Chong, L.; Lee, M.; Lee, T.; Duan, Y.; Wang, W.; Donini, O.; Cieplak, P.; Srinivasan, J.; Case, D.A.; Cheatham, T.E., III Calculating structures and free energies of complex molecules: combining molecular mechanics and continuum models. *Acc. Chem. Res.,* **2000**, *33*(12), 889-897. http://dx.doi.org/10.1021/ar000033j PMID: 11123888

[63] Genheden, S.; Ryde, U. Comparison of end-point continuum-solvation methods for the calculation of protein-ligand binding free energies. *Proteins,* **2012**, *80*(5), 1326-1342. http://dx.doi.org/10.1002/prot.24029 PMID: 22274991

[64] Mobley, D.L.; Dill, K.A.; Chodera, J.D. Treating entropy and conformational changes in implicit solvent simulations of small molecules. *J. Phys. Chem. B,* **2008**, *112*(3), 938-946. http://dx.doi.org/10.1021/jp0764384 PMID: 18171044

[65] Vicatos, S.; Roca, M.; Warshel, A. Effective approach for calculations of absolute stability of proteins using focused dielectric constants. *Proteins,* **2009**, *77*(3), 670-684. http://dx.doi.org/10.1002/prot.22481 PMID: 19856460

[66] Dominy, B.N.; Minoux, H.; Brooks, C.L., III An electrostatic basis for the stability of thermophilic proteins. *Proteins,* **2004**, *57*(1), 128-141. http://dx.doi.org/10.1002/prot.20190 PMID: 15326599

[67] Chakravorty, A.; Panday, S.; Pahari, S.; Zhao, S.; Alexov, E. Capturing the effects of explicit waters in implicit electrostatics modeling: qualitative justification of Gaussian-based dielectric models in DelPhi. *J. Chem. Inf. Model.,* **2020**, *60*(4), 2229-2246. http://dx.doi.org/10.1021/acs.jcim.0c00151 PMID: 32155062

[68] Fu, L.; Ye, F.; Feng, Y.; Yu, F.; Wang, Q.; Wu, Y.; Zhao, C.; Sun, H.; Huang, B.; Niu, P.; Song, H.; Shi, Y.; Li, X.; Tan, W.; Qi, J.; Gao, G.F. Both boceprevir and GC376 efficaciously inhibit SARS-CoV-2 by targeting its main protease. *Nat. Commun.,* **2020**, *11*(1), 4417. http://dx.doi.org/10.1038/s41467-020-18233-x PMID: 32887884

[69] de Azevedo, W.F. Jr.; Canduri, F.; Basso, L.A.; Palma, M.S.; Santos, D.S. Determining the structural basis for specificity of ligands using crystallographic screening. *Cell Biochem. Biophys.,* **2006**, *44*(3), 405-411. http://dx.doi.org/10.1385/CBB:44:3:405 PMID: 16679527

[70] Canduri, F.; de Azevedo, W.F. Protein crystallography in drug discovery. *Curr. Drug Targets,* **2008**, *9*(12), 1048-1053. http://dx.doi.org/10.2174/138945008786949423 PMID: 19128214

[71] Canduri, F.; Silva, R.G.; dos Santos, D.M.; Palma, M.S.; Basso, L.A.; Santos, D.S.; de Azevedo, W.F. Jr. Structure of human PNP complexed with ligands. *Acta Crystallogr. D Biol. Crystallogr.,* **2005**, *61*(Pt 7), 856-862. http://dx.doi.org/10.1107/S0907444905005421 PMID: 15983407

[72] Delatorre, P.; de Azevedo, W.F. Jr. Simulation of electron density maps for two-dimensional crystal structures using Mathematica. *J. Appl. Cryst.,* **2001**, *34*(5), 658-660. http://dx.doi.org/10.1107/S0021889801009724

[73] Bitencourt-Ferreira, G.; Veit-Acosta, M.; de Azevedo, W.F.Jr. Van der waals potential in protein complexes. *Methods Mol. Biol.,* **2019**, *2053*, 79-91. http://dx.doi.org/10.1007/978-1-4939-9752-7_6 PMID: 31452100

[74] Bitencourt-Ferreira, G.; Veit-Acosta, M.; de Azevedo, W.F. Jr. Electrostatic energy in protein-ligand complexes. *Methods Mol. Biol.,* **2019**, *2053*, 67-77. http://dx.doi.org/10.1007/978-1-4939-9752-7_5 PMID: 31452099

[75] Bitencourt-Ferreira, G.; Veit-Acosta, M.; de Azevedo, W.F. Jr. Hydrogen bonds in protein-ligand complexes. *Methods Mol. Biol.,* **2019**, *2053*, 93-107. http://dx.doi.org/10.1007/978-1-4939-9752-7_7 PMID: 31452101

[76] De Azevedo, W.F. Jr.; Leclerc, S.; Meijer, L.; Havlicek, L.; Strnad, M.; Kim, S.H. Inhibition of cyclin-dependent kinases by purine analogues: crystal structure of human cdk2 complexed with roscovitine. *Eur. J. Biochem.,* **1997**, *243*(1-2), 518-526. http://dx.doi.org/10.1111/j.1432-1033.1997.0518a.x PMID: 9030780

[77] De Azevedo, W.F. Jr.; Mueller-Dieckmann, H.J.; Schulze-Gahmen, U.; Worland, P.J.; Sausville, E.; Kim, S.H. Structural basis for specificity and potency of a flavonoid inhibitor of human CDK2, a cell cycle kinase. *Proc. Natl. Acad. Sci. USA,* **1996**, *93*(7), 2735-2740. http://dx.doi.org/10.1073/pnas.93.7.2735 PMID: 8610110

[78] Canduri, F.; Teodoro, L.G.; Fadel, V.; Lorenzi, C.C.; Hial, V.; Gomes, R.A.; Neto, J.R.; de Azevedo, W.F. Jr. Structure of human uropepsin at 2.45 Å resolution. *Acta Crystallogr. D Biol. Crystallogr.,* **2001**, *57*(Pt 11), 1560-1570. http://dx.doi.org/10.1107/S0907444901013865 PMID: 11679720

[79] de Azevedo, W.F. Jr.; Canduri, F.; da Silveira, N.J. Structural basis for inhibition of cyclin-dependent kinase 9 by flavopiridol. *Biochem. Biophys. Res. Commun.,* **2002**,

293(1), 566-571.
http://dx.doi.org/10.1016/S0006-291X(02)00266-8 PMID: 12054639

[80] Filgueira de Azevedo, W.Jr.; Gaspar, R.T.; Canduri, F.; Camera, J.C.Jr.; Freitas da Silveira, N.J. Molecular model of cyclin-dependent kinase 5 complexed with roscovitine. *Biochem. Biophys. Res. Commun.,* **2002**, *297*(5), 1154-1158.
http://dx.doi.org/10.1016/S0006-291X(02)02352-5 PMID: 12372407

[81] Sulimov, V.B.; Kutov, D.C.; Sulimov, A.V. Advances in Docking. *Curr. Med. Chem.,* **2019**, *26*(42), 7555-7580.
http://dx.doi.org/10.2174/0929867325666180904115000 PMID: 30182836

[82] Gally, J.M.; Bourg, S.; Fogha, J.; Do, Q.T.; Aci-Sèche, S.; Bonnet, P. VSPrep: A KNIME workflow for the preparation of molecular databases for virtual screening. *Curr. Med. Chem.,* **2020**, *27*(38), 6480-6494.
http://dx.doi.org/10.2174/0929867326666190614160451 PMID: 31242833

[83] Kim, C.; Kim, E. Rational drug design approach of receptor tyrosine kinase type III inhibitors. *Curr. Med. Chem.,* **2019**, *26*(42), 7623-7640.
http://dx.doi.org/10.2174/0929867325666180622143548 PMID: 29932031

[84] Hu, X.; Maffucci, I.; Contini, A. Advances in the treatment of explicit water molecules in docking and binding free energy calculations. *Curr. Med. Chem.,* **2019**, *26*(42), 7598-7622.
http://dx.doi.org/10.2174/0929867325666180514110824 PMID: 29756561

[85] Potemkin, V.; Grishina, M. Grid-based technologies for *in silico* screening and drug design. *Curr. Med. Chem.,* **2018**, *25*(29), 3526-3537.
http://dx.doi.org/10.2174/0929867325666180309112454 PMID: 29521207

[86] Azevedo, L.S.; Moraes, F.P.; Xavier, M.M.; Pantoja, E.O.; Villavicencio, B.; Finck, J.A.; Proenca, A.M.; Rocha, K.B.; de Azevedo, W. F. Jr. Recent progress of molecular docking simulations applied to development of drugs. *Curr. Bioinform.,* **2012**, *7*(4), 352-365.
http://dx.doi.org/10.2174/157489312803901063

[87] Liu, X.; Zhu, F.; Ma, X.H.; Shi, Z.; Yang, S.Y.; Wei, Y.Q.; Chen, Y.Z. Predicting targeted polypharmacology for drug repositioning and multi- target drug discovery. *Curr. Med. Chem.,* **2013**, *20*(13), 1646-1661.
http://dx.doi.org/10.2174/0929867311320130005 PMID: 23410165

[88] Musella, S.; Verna, G.; Fasano, A.; Di Micco, S. New perspectives of machine learning in drug discovery. *Curr. Med. Chem.,* **2021**, *28*(32), 6704-6728.
http://dx.doi.org/10.2174/0929867327666201111144048 PMID: 33176630

[89] Abbasi, K.; Razzaghi, P.; Poso, A.; Ghanbari-Ara, S.; Masoudi-Nejad, A. Deep learning in drug target interaction prediction: current and future perspective. *Curr. Med. Chem.,* **2021**, *28*(11), 2100-2113.
http://dx.doi.org/10.2174/0929867327666200907141016 PMID: 32895036

[90] Bruno, A.; Costantino, G.; Sartori, L.; Radi, M. The *in silico* drug discovery toolbox: applications in lead discovery and optimization. *Curr. Med. Chem.,* **2019**, *26*(21), 3838-3873.
http://dx.doi.org/10.2174/0929867324666171107101035 PMID: 29110597

[91] Lohning, A.E.; Levonis, S.M.; Williams-Noonan, B.; Schweiker, S.S. A practical guide to molecular docking and homology modelling for medicinal chemists. *Curr. Top. Med. Chem.,* **2017**, *17*(18), 2023-2040.
http://dx.doi.org/10.2174/1568026617666170130110827 PMID: 28137238

[92] Forrestall, K.L.; Burley, D.E.; Cash, M.K.; Pottie, I.R.; Darvesh, S. 2-pyridone natural products as inhibitors of SARS-CoV-2 main protease. *Chem. Biol. Interact.,* **2021**, *335*, 1009348.
http://dx.doi.org/10.1016/j.cbi.2020.109348 PMID: 33278462

[93] Rehman, M.T.; AlAjmi, M.F.; Hussain, A. Natural compounds as inhibitors of SARS-CoV-2 main protease ($3CL^{pro}$): a molecular docking and simulation approach to combat COVID-19. *Curr. Pharm. Des.,* **2021**, *27*(33), 3577-3589.
http://dx.doi.org/10.2174/1381612826999201116195851 PMID: 33200697

[94] Garg, S.; Roy, A. *In silico* analysis of selected alkaloids against main protease (M^{pro}) of SARS-CoV-2. *Chem. Biol. Interact.,* **2020**, *332*, 109309.
http://dx.doi.org/10.1016/j.cbi.2020.109309 PMID: 33181114

[95] Ragavan Rameshkumar, M.; Indu, P.; Arunagirinathan, N.; Venkatadri, B.; El-Serehy, H.A.; Ahmad, A. Computational selection of flavonoid compounds as inhibitors against SARS-CoV-2 main protease, RNA-dependent RNA polymerase and spike proteins: a molecular docking study. *Saudi J. Biol. Sci.,* **2021**, *28*(1), 448-458.
http://dx.doi.org/10.1016/j.sjbs.2020.10.028 PMID: 33110386

[96] C, S.; S, D.K.; Ragunathan, V.; Tiwari, P.; A, S.; P, B.D. Molecular docking, validation, dynamics simulations, and pharmacokinetic prediction of natural compounds against the SARS-CoV-2 main-protease. *J. Biomol. Struct. Dyn.,* **2020**, *8*, 1-27.
http://dx.doi.org/10.1080/07391102.2020.1815584 PMID: 32897178

[97] Majumder, R.; Mandal, M. Screening of plant-based natural compounds as a potential COVID-19 main protease inhibitor: an *in silico* docking and molecular dynamics simulation approach. *J. Biomol. Struct. Dyn.,* **2020**, *8*, 1-16.
http://dx.doi.org/10.1080/07391102.2020.1817787 PMID: 32897138

[98] Maiti, S.; Banerjee, A.; Nazmeen, A.; Kanwar, M.; Das, S. Active-site molecular docking of nigellidine with nucleocapsid- NSP2-MPro of COVID-19 and to human IL1R-IL6R and strong antioxidant role of *Nigella-sativa* in experimental rats. *J. Drug Target.,* **2020**, *2*, 1-23.
http://dx.doi.org/10.1080/1061186X.2020.1817040 PMID: 32875925

[99] Kundu, D.; Selvaraj, C.; Singh, S.K.; Dubey, V.K. Identification of new anti-nCoV drug chemical compounds from Indian spices exploiting SARS-CoV-2 main protease as target. *J. Biomol. Struct. Dyn.,* **2021**, *39*(9), 3428-3434.
http://dx.doi.org/10.1080/07391102.2020.1763202 PMID: 32362243

[100] Bitencourt-Ferreira, G.; de Azevedo, W.F. Jr. How docking programs work. *Methods Mol. Biol.,* **2019**, *2053*, 35-50.
http://dx.doi.org/10.1007/978-1-4939-9752-7_3 PMID: 31452097

[101] Jin, Z.; Du, X.; Xu, Y.; Deng, Y.; Liu, M.; Zhao, Y.; Zhang, B.; Li, X.; Zhang, L.; Peng, C.; Duan, Y.; Yu, J.;

Wang, L.; Yang, K.; Liu, F.; Jiang, R.; Yang, X.; You, T.; Liu, X.; Yang, X.; Bai, F.; Liu, H.; Liu, X.; Guddat, L.W.; Xu, W.; Xiao, G.; Qin, C.; Shi, Z.; Jiang, H.; Rao, Z.; Yang, H. Structure of M^{pro} from SARS-CoV-2 and discovery of its inhibitors. *Nature,* **2020**, *582*(7811), 289-293. http://dx.doi.org/10.1038/s41586-020-2223-y PMID: 32272481

[102] Kneller, D.W.; Phillips, G.; O'Neill, H.M.; Jedrzejczak, R.; Stols, L.; Langan, P.; Joachimiak, A.; Coates, L.; Kovalevsky, A. Structural plasticity of SARS-CoV-2 3CL M^{pro} active site cavity revealed by room temperature X-ray crystallography. *Nat. Commun.,* **2020**, *11*(1), 3202. http://dx.doi.org/10.1038/s41467-020-16954-7 PMID: 32581217

[103] Gentile, D.; Patamia, V.; Scala, A.; Sciortino, M.T.; Piperno, A.; Rescifina, A. Putative inhibitors of SARS-CoV-2 main protease from a library of marine natural products: a virtual screening and molecular modeling study. *Mar. Drugs,* **2020**, *18*(4), 225. http://dx.doi.org/10.3390/md18040225 PMID: 32340389

[104] Trott, O.; Olson, A.J. AutoDock vina: improving the speed and accuracy of docking with a new scoring function, efficient optimization, and multithreading. *J. Comput. Chem.,* **2010**, *31*(2), 455-461. http://dx.doi.org/10.1002/jcc.21334 PMID: 19499576

[105] Heck, G.S.; Pintro, V.O.; Pereira, R.R.; de Ávila, M.B.; Levin, N.M.B.; de Azevedo, W.F. Supervised machine learning methods applied to predict ligand-binding affinity. *Curr. Med. Chem.,* **2017**, *24*(23), 2459-2470. http://dx.doi.org/10.2174/0929867324666170623092503 PMID: 28641555

[106] Batool, M.; Ahmad, B.; Choi, S. A structure-based drug discovery paradigm. *Int. J. Mol. Sci.,* **2019**, *20*(11), 2783. http://dx.doi.org/10.3390/ijms20112783 PMID: 31174387

[107] Li, J.; Fu, A.; Zhang, L. An overview of scoring functions used for protein-ligand interactions in molecular docking. *Interdiscip. Sci.,* **2019**, *11*(2), 320-328. http://dx.doi.org/10.1007/s12539-019-00327-w PMID: 30877639

[108] Li, F.; Wang, Y.; Li, C.; Marquez-Lago, T.T.; Leier, A.; Rawlings, N.D.; Haffari, G.; Revote, J.; Akutsu, T.; Chou, K.C.; Purcell, A.W.; Pike, R.N.; Webb, G.I.; Ian Smith, A.; Lithgow, T.; Daly, R.J.; Whisstock, J.C.; Song, J. Twenty years of bioinformatics research for protease-specific substrate and cleavage site prediction: a comprehensive revisit and benchmarking of existing methods. *Brief. Bioinform.,* **2019**, *20*(6), 2150-2166. http://dx.doi.org/10.1093/bib/bby077 PMID: 30184176

[109] Bitencourt-Ferreira, G.; de Azevedo, W.F. Jr. Machine learning to predict binding affinity. *Methods Mol. Biol.,* **2019**, *2053*, 251-273. http://dx.doi.org/10.1007/978-1-4939-9752-7_16 PMID: 31452110

[110] Bitencourt-Ferreira, G.; de Azevedo, W.F. Jr. Exploring the scoring function space. *Methods Mol. Biol.,* **2019**, *2053*, 275-281. http://dx.doi.org/10.1007/978-1-4939-9752-7_17 PMID: 31452111

[111] Fresnais, L.; Ballester, P.J. The impact of compound library size on the performance of scoring functions for structure-based virtual screening. *Brief. Bioinform.,* **2021**, *22*(3), bbaa095. http://dx.doi.org/10.1093/bib/bbaa095 PMID: 32568385

[112] Xiong, G.L.; Ye, W.L.; Shen, C.; Lu, A.P.; Hou, T.J.; Cao, D.S. Improving structure-based virtual screening performance *via* learning from scoring function components. *Brief. Bioinform.,* **2021**, *22*(3), bbaa094. http://dx.doi.org/10.1093/bib/bbaa094 PMID: 32496540

[113] Olson, A.J.; Goodsell, D.S. Automated docking and the search for HIV protease inhibitors. *SAR QSAR Environ. Res.,* **1998**, *8*(3-4), 273-285. http://dx.doi.org/10.1080/10629369808039144 PMID: 9522477

[114] Berti, F.; Frecer, V.; Miertus, S. Inhibitors of HIV-protease from computational design. A history of theory and synthesis still to be fully appreciated. *Curr. Pharm. Des.,* **2014**, *20*(21), 3398-3411. http://dx.doi.org/10.2174/13816128113199990628 PMID: 24001234

[115] Li, H.; Peng, J.; Sidorov, P.; Leung, Y.; Leung, K.S.; Wong, M.H.; Lu, G.; Ballester, P.J. Classical scoring functions for docking are unable to exploit large volumes of structural and interaction data. *Bioinformatics,* **2019**, *35*(20), 3989-3995. http://dx.doi.org/10.1093/bioinformatics/btz183 PMID: 30873528

[116] Seifert, M.H. Targeted scoring functions for virtual screening. *Drug Discov. Today,* **2009**, *14*(11-12), 562-569. http://dx.doi.org/10.1016/j.drudis.2009.03.013 PMID: 19508918

[117] Pinzi, L.; Rastelli, G. Molecular docking: shifting paradigms in drug discovery. *Int. J. Mol. Sci.,* **2019**, *20*(18), 4331. http://dx.doi.org/10.3390/ijms20184331 PMID: 31487867

[118] Trosset, J.Y.; Cavé, C. *In silico* drug-target profiling. *Methods Mol. Biol.,* **2019**, *1953*, 89-103. http://dx.doi.org/10.1007/978-1-4939-9145-7_6 PMID: 30912017

[119] Dinić, J.; Efferth, T.; García-Sosa, A.T.; Grahovac, J.; Padrón, J.M.; Pajeva, I.; Rizzolio, F.; Saponara, S.; Spengler, G.; Tsakovska, I. Repurposing old drugs to fight multidrug resistant cancers. *Drug Resist. Updat.,* **2020**, *52*, 100713. http://dx.doi.org/10.1016/j.drup.2020.100713 PMID: 32615525

[120] Shanmugam, A.; Muralidharan, N.; Velmurugan, D.; Gromiha, M.M. Therapeutic targets and computational approaches on drug development for COVID-19. *Curr. Top. Med. Chem.,* **2020**, *20*(24), 2210-2220. http://dx.doi.org/10.2174/1568026620666200710105507 PMID: 32648845

[121] Gns, H.S.; Gr, S.; Murahari, M.; Krishnamurthy, M. An update on Drug Repurposing: Re-written saga of the drug's fate. *Biomed. Pharmacother.,* **2019**, *110*, 700-716. http://dx.doi.org/10.1016/j.biopha.2018.11.127 PMID: 30553197

[122] Bitencourt-Ferreira, G.; de Azevedo, W.F. Jr. Homology modeling of protein targets with MODELLER. *Methods Mol. Biol.,* **2019**, *2053*, 231-249. http://dx.doi.org/10.1007/978-1-4939-9752-7_15 PMID: 31452109

[123] Sali, A.; Blundell, T.L. Comparative protein modelling by satisfaction of spatial restraints. *J. Mol. Biol.,* **1993**, *234*(3), 779-815. http://dx.doi.org/10.1006/jmbi.1993.1626 PMID: 8254673

[124] Uchôa, H.B.; Jorge, G.E.; Freitas Da Silveira, N.J.; Camera, J.C. Jr.; Canduri, F.; De Azevedo, W.F. Jr. Parmodel: a web server for automated comparative modeling of proteins. *Biochem. Biophys. Res. Commun.,* **2004**, *325*(4), 1481-1486. http://dx.doi.org/10.1016/j.bbrc.2004.10.192 PMID:

15555595

[125] Zar, J. Significance testing of the Spearman rank correlation coefficient. *J. Am. Stat. Assoc.,* **1972**, *67*(339), 578-580. http://dx.doi.org/10.1080/01621459.1972.10481251

[126] Falavigna, M.; Colpani, V.; Stein, C.; Azevedo, L.C.P.; Bagattini, A.M.; Brito, G.V.; Chatkin, J.M.; Cimerman, S.; Corradi, M.F.D.B.; Cunha, C.A.D.; Medeiros, F.C.; Oliveira Junior, H.A.; Fritscher, L.G.; Gazzana, M.B.; Gräf, D.D.; Marra, L.P.; Matuoka, J.Y.; Nunes, M.S.; Pachito, D.V.; Pagano, C.G.M.; Parreira, P.C.S.; Riera, R.; Silva, A. Jr.; Tavares, B.M.; Zavascki, A.P.; Rosa, R.G.; Dal-Pizzol, F. Guidelines for the pharmacological treatment of COVID-19. The task-force/consensus guideline of the Brazilian association of intensive care medicine, the Brazilian society of infectious diseases and the Brazilian society of pulmonology and tisiology. *Rev. Bras. Ter. Intensiva,* **2020**, *32*(2), 166-196. http://dx.doi.org/10.5935/0103-507x.20200039 PMID: 32667444

[127] AlQuraishi, M. AlphaFold at CASP13. *Bioinformatics,* **2019**, *35*(22), 4862-4865. http://dx.doi.org/10.1093/bioinformatics/btz422 PMID: 31116374

[128] Heo, L.; Feig, M. High-accuracy protein structures by combining machine-learning with physics-based refinement. *Proteins,* **2020**, *88*(5), 637-642. http://dx.doi.org/10.1002/prot.25847 PMID: 31693199

[129] Senior, A.W.; Evans, R.; Jumper, J.; Kirkpatrick, J.; Sifre, L.; Green, T.; Qin, C.; Žídek, A.; Nelson, A.W.R.; Bridgland, A.; Penedones, H.; Petersen, S.; Simonyan, K.; Crossan, S.; Kohli, P.; Jones, D.T.; Silver, D.; Kavukcuoglu, K.; Hassabis, D. Protein structure prediction using multiple deep neural networks in the 13th critical assessment of protein structure prediction (CASP13). *Proteins,* **2019**, *87*(12), 1141-1148. http://dx.doi.org/10.1002/prot.25834 PMID: 31602685

[130] Thomsen, R.; Christensen, M.H. MolDock: a new technique for high-accuracy molecular docking. *J. Med. Chem.,* **2006**, *49*(11), 3315-3321. http://dx.doi.org/10.1021/jm051197e PMID: 16722650

[131] Heberlé, G.; de Azevedo, W.F. Jr. Bio-inspired algorithms applied to molecular docking simulations. *Curr. Med. Chem.,* **2011**, *18*(9), 1339-1352. http://dx.doi.org/10.2174/092986711795029573 PMID: 21366530

[132] Bitencourt-Ferreira, G.; de Azevedo, W.F. Jr. Molegro virtual docker for docking. *Methods Mol. Biol.,* **2019**, *2053*, 149-167. http://dx.doi.org/10.1007/978-1-4939-9752-7_10 PMID: 31452104

[133] Stepniewska-Dziubinska, M.M.; Zielenkiewicz, P.; Siedlecki, P. Development and evaluation of a deep learning model for protein-ligand binding affinity prediction. *Bioinformatics,* **2018**, *34*(21), 3666-3674. http://dx.doi.org/10.1093/bioinformatics/bty374 PMID: 29757353

[134] Das, S.; Krein, M.P.; Breneman, C.M. Binding affinity prediction with property-encoded shape distribution signatures. *J. Chem. Inf. Model.,* **2010**, *50*(2), 298-308. http://dx.doi.org/10.1021/ci9004139 PMID: 20095526

[135] Durrant, J.D.; McCammon, J.A. NNScore: a neural-network-based scoring function for the characterization of protein-ligand complexes. *J. Chem. Inf. Model.,* **2010**, *50*(10), 1865-1871. http://dx.doi.org/10.1021/ci100244v PMID: 20845954

[136] Durrant, J.D.; McCammon, J.A. NNScore 2.0: a neural-network receptor-ligand scoring function. *J. Chem. Inf. Model.,* **2011**, *51*(11), 2897-2903. http://dx.doi.org/10.1021/ci2003889 PMID: 22017367

[137] Durrant, J.D.; Friedman, A.J.; Rogers, K.E.; McCammon, J.A. Comparing neural-network scoring functions and the state of the art: applications to common library screening. *J. Chem. Inf. Model.,* **2013**, *53*(7), 1726-1735. http://dx.doi.org/10.1021/ci400042y PMID: 23734946

[138] Sterling, T.; Irwin, J.J. ZINC 15-ligand discovery for everyone. *J. Chem. Inf. Model.,* **2015**, *55*(11), 2324-2337. http://dx.doi.org/10.1021/acs.jcim.5b00559 PMID: 26479676

[139] Irwin, J.J.; Sterling, T.; Mysinger, M.M.; Bolstad, E.S.; Coleman, R.G. ZINC: a free tool to discover chemistry for biology. *J. Chem. Inf. Model.,* **2012**, *52*(7), 1757-1768. http://dx.doi.org/10.1021/ci3001277 PMID: 22587354

[140] Irwin, J.J.; Shoichet, B.K. ZINC--a free database of commercially available compounds for virtual screening. *J. Chem. Inf. Model.,* **2005**, *45*(1), 177-182. http://dx.doi.org/10.1021/ci049714+ PMID: 15667143

[141] Santos, L.H.S.; Ferreira, R.S.; Caffarena, E.R. Integrating molecular docking and molecular dynamics simulations. *Methods Mol. Biol.,* **2019**, *2053*, 13-34. http://dx.doi.org/10.1007/978-1-4939-9752-7_2 PMID: 31452096

[142] van der Spoel, D.; van Maaren, P.J.; Caleman, C. GROMACS molecule & liquid database. *Bioinformatics,* **2012**, *28*(5), 752-753. http://dx.doi.org/10.1093/bioinformatics/bts020 PMID: 22238269

[143] Sanbonmatsu, K.Y.; Tung, C.S. High performance computing in biology: multimillion atom simulations of nanoscale systems. *J. Struct. Biol.,* **2007**, *157*(3), 470-480. http://dx.doi.org/10.1016/j.jsb.2006.10.023 PMID: 17187988

[144] Bitencourt-Ferreira, G.; de Azevedo, W.F. Jr. Molecular dynamics simulations with NAMD2. *Methods Mol. Biol.,* **2019**, *2053*, 109-124. http://dx.doi.org/10.1007/978-1-4939-9752-7_8 PMID: 31452102

[145] de Azevedo, W.F. Jr. Molecular dynamics simulations of protein targets identified in *Mycobacterium tuberculosis*. *Curr. Med. Chem.,* **2011**, *18*(9), 1353-1366. http://dx.doi.org/10.2174/092986711795029519 PMID: 21366529

[146] Gasteiger, J.; Marsili, M. A new model for calculating atomic charges in molecules. *Tetrahedron Lett.,* **1978**, *19*(34), 3181-3184. http://dx.doi.org/10.1016/S0040-4039(01)94977-9

[147] Gasteiger, J.; Marsili, M. Iterative partial equalization of orbital electronegativity—a rapid access to atomic charges. *Tetrahedron,* **1980**, *36*(22), 3219-3228. http://dx.doi.org/10.1016/0040-4020(80)80168-2

[148] Bitencourt-Ferreira, G.; de Azevedo Junior, W.F. Electrostatic potential energy in protein-drug complexes. *Curr. Med. Chem.,* **2021**, *28*(24), 4954-4971. http://dx.doi.org/10.2174/0929867328666210201150842 PMID: 33593246

[149] Hejazi, I.I.; Beg, M.A.; Imam, M.A.; Athar, F.; Islam, A. Glossary of phytoconstituents: can these be repurposed against SARS CoV-2? A quick *in silico* screening of various phytoconstituents from plant *Glycyrrhiza glabra* with SARS CoV-2 main protease. *Food Chem. Toxicol.,* **2021**,

150, 112057.
http://dx.doi.org/10.1016/j.fct.2021.112057 PMID: 33592201

[150] Aydın, A.D.; Altınel, F.; Erdoğmuş, H.; Son, Ç.D. Allergen fragrance molecules: a potential relief for COVID-19. *BMC Complement Med. Ther.,* **2021**, *21*(1), 41.
http://dx.doi.org/10.1186/s12906-021-03214-4 PMID: 33478471

[151] Kwofie, S.K.; Broni, E.; Asiedu, S.O.; Kwarko, G.B.; Dankwa, B.; Enninful, K.S.; Tiburu, E.K.; Wilson, M.D. Cheminformatics-based identification of potential novel anti-SARS-CoV-2 natural compounds of African origin. *Molecules,* **2021**, *26*(2), 406.
http://dx.doi.org/10.3390/molecules26020406 PMID: 33466743

[152] Thangavel, N.; Al Bratty, M.; Al Hazmi, H.A.; Najmi, A.; Ali Alaqi, R.O. Silico evaluation of prospective anti--COVID-19 drug candidates as potential SARS-CoV-2 main protease inhibitors. *Protein J.,* **2021**, *40*(3), 296-309.
http://dx.doi.org/10.1007/s10930-020-09945-6

[153] Ibrahim, M.A.A.; Abdelrahman, A.H.M.; Allemailem, K.S.; Almatroudi, A.; Moustafa, M.F.; Hegazy, M.F. *In silico* evaluation of prospective anti-COVID-19 drug candidates as potential SARS-CoV-2 main protease inhibitors. *Protein J.,* **2021**, *40*(3), 269-309.
http://dx.doi.org/10.1007/s10930-020-09945-6 PMID: 33387249

[154] Tallei, T.E.; Tumilaar, S.G.; Niode, N.J.; Fatimawali; Kepel, B.J.; Idroes, R.; Effendi, Y.; Sakib, S.A.; Emran, T.B. Potential of plant bioactive compounds as SARS-CoV-2 main protease (M^{pro}) and spike (S) glycoprotein inhibitors: a molecular docking study. *Scientifica (Cairo),* **2020**, *2020*, 6307457.
http://dx.doi.org/10.1155/2020/6307457 PMID: 33425427

[155] Jamalan, M.; Barzegari, E.; Gholami-Borujeni, F. Structure-based screening to discover new inhibitors for papain--like proteinase of SARS-CoV-2: an *In silico* study. *J. Proteome Res.,* **2021**, *20*(1), 1015-1026.
http://dx.doi.org/10.1021/acs.jproteome.0c00836 PMID: 33350309

[156] Abdusalam, A.A.A.; Murugaiyah, V. Identification of potential inhibitors of 3CL protease of SARS-CoV-2 from Zinc database by molecular docking-based virtual screening. *Front. Mol. Biosci.,* **2020**, *7*, 603037.
http://dx.doi.org/10.3389/fmolb.2020.603037 PMID: 33392261

[157] Mohamed, K.; Yazdanpanah, N.; Saghazadeh, A.; Rezaei, N. Computational drug discovery and repurposing for the treatment of COVID-19: a systematic review. *Bioorg. Chem.,* **2021**, *106*, 104490.
http://dx.doi.org/10.1016/j.bioorg.2020.104490 PMID: 33261845

[158] Mhatre, S.; Naik, S.; Patravale, V. A molecular docking study of EGCG and theaflavin digallate with the druggable targets of SARS-CoV-2. *Comput. Biol. Med.,* **2021**, *129*, 104137.
http://dx.doi.org/10.1016/j.compbiomed.2020.104137 PMID: 33302163

[159] Tachoua, W.; Kabrine, M.; Mushtaq, M.; Ul-Haq, Z. An *in--silico* evaluation of COVID-19 main protease with clinically approved drugs. *J. Mol. Graph. Model.,* **2020**, *101*, 107758.
http://dx.doi.org/10.1016/j.jmgm.2020.107758 PMID: 33007575

[160] Shah, V.R.; Bhaliya, J.D.; Patel, G.M. *In silico* approach: docking study of oxindole derivatives against the main protease of COVID-19 and its comparison with existing therapeutic agents. *J. Basic Clin. Physiol. Pharmacol.,* **2021**, *32*(3), 197-214.
http://dx.doi.org/10.1515/jbcpp-2020-0262 PMID: 33594850

[161] Absalan, A.; Doroud, D.; Salehi-Vaziri, M.; Kaghazian, H.; Ahmadi, N.; Zali, F.; Pouriavali's, M.H.; Mousavi--Nasab, S.D. Computation screening and molecular docking of FDA approved viral protease inhibitors as a potential drug against COVID-19. *Gastroenterol. Hepatol. Bed Bench,* **2020**, *13*(4), 355-360.
PMID: 33244378

[162] Dubey, R.; Dubey, K. Molecular docking studies of bioactive nicotiflorin against 6W63 novel coronavirus 2019 (COVID-19). *Comb. Chem. High Throughput Screen.,* **2021**, *24*(6), 874-878.
http://dx.doi.org/10.2174/1386207323999200820162551 PMID: 33109057

[163] Veit-Acosta, M.; de Azevedo Junior, W.F. The impact of crystallographic data for the development of machine learning models to predict protein-ligand binding affinity. *Curr. Med. Chem.,* **2021**. Epub Ahead of Print
http://dx.doi.org/10.2174/0929867328666210210121320 PMID: 33568025

[164] Elekofehinti, O.O.; Iwaloye, O.; Josiah, S.S.; Lawal, A.O.; Akinjiyan, M.O.; Ariyo, E.O. Molecular docking studies, molecular dynamics and ADME/tox reveal therapeutic potentials of STOCK1N-69160 against papain-like protease of SARS-CoV-2. *Mol. Divers.,* **2021**, *25*(3), 1761-1773.
http://dx.doi.org/10.1007/s11030-020-10151-w PMID: 33201386

[165] Dahab, M.A.; Hegazy, M.M.; Abbass, H.S. Hordatines as a potential inhibitor of COVID-19 main protease and RNA polymerase: an *in-silico* approach. *Nat. Prod. Bioprospect.,* **2020**, *10*(6), 453-462.
http://dx.doi.org/10.1007/s13659-020-00275-9 PMID: 33090359

[166] Chikhale, R.V.; Gupta, V.K.; Eldesoky, G.E.; Wabaidur, S.M.; Patil, S.A.; Islam, M.A. Identification of potential anti-TMPRSS2 natural products through homology modelling, virtual screening and molecular dynamics simulation studies. *J. Biomol. Struct. Dyn.,* **2020**, 1-16. Online ahead of print.
http://dx.doi.org/10.1080/07391102.2020.1798813 PMID: 32741259

[167] Maurya, S.K.; Maurya, A.K.; Mishra, N.; Siddique, H.R. Virtual screening, ADME/T, and binding free energy analysis of anti-viral, anti-protease, and anti-infectious compounds against NSP10/NSP16 methyltransferase and main protease of SARS CoV-2. *J. Recept. Signal Transduct. Res.,* **2020**, *40*(6), 605-612.
http://dx.doi.org/10.1080/10799893.2020.1772298 PMID: 32476594

[168] Khan, M.T.; Ali, A.; Wang, Q.; Irfan, M.; Khan, A.; Zeb, M.T.; Zhang, Y.J.; Chinnasamy, S.; Wei, D.Q. Marine natural compounds as potents inhibitors against the main protease of SARS-CoV-2-a molecular dynamic study. *J. Biomol. Struct. Dyn.,* **2021**, *39*(10), 3627-3637.
http://dx.doi.org/10.1080/07391102.2020.1769733 PMID: 32410504

[169] Peele, K.A.; Durthi, C.P.; Srihansa, T.; Krupanidhi, S.; Ayyagari, V.S.; Babu, D.J.; Indira, M.; Reddy, A.R.; Venkateswarulu, T.C. Molecular docking and dynamic simulations for antiviral compounds against SARS-CoV-2: a

computational study. *Inform. Med. Unlocked,* **2020**, *19*, 100345.
http://dx.doi.org/10.1016/j.imu.2020.100345 PMID: 32395606

[170] Gao, F.; Ou, H.Y.; Chen, L.L.; Zheng, W.X.; Zhang, C.T. Prediction of proteinase cleavage sites in polyproteins of coronaviruses and its applications in analyzing SARS-CoV genomes. *FEBS Lett.,* **2003**, *553*(3), 451-456.
http://dx.doi.org/10.1016/S0014-5793(03)01091-3 PMID: 14572668

[171] Kabra, R.; Singh, S. Evolutionary artificial intelligence based peptide discoveries for effective Covid-19 therapeutics. *Biochim. Biophys. Acta Mol. Basis Dis.,* **2021**, *1867*(1), 165978.
http://dx.doi.org/10.1016/j.bbadis.2020.165978 PMID: 32980462

[172] Rai, H.; Barik, A.; Singh, Y.P.; Suresh, A.; Singh, L.; Singh, G.; Nayak, U.Y.; Dubey, V.K.; Modi, G. Molecular docking, binding mode analysis, molecular dynamics, and prediction of ADMET/toxicity properties of selective potential antiviral agents against SARS-CoV-2 main protease: an effort toward drug repurposing to combat COVID-19. *Mol. Divers.,* **2021**, *25*(3), 1905-1927.
http://dx.doi.org/10.1007/s11030-021-10188-5 PMID: 33582935

[173] Scior, T.; Abdallah, H.H.; Mustafa, S.F.Z.; Guevara-García, J.A.; Rehder, D. Are vanadium complexes druggable against the main protease M^{pro} of SARS-CoV-2? - A computational approach. *Inorg. Chim. Acta,* **2021**, *519*, 120287.
http://dx.doi.org/10.1016/j.ica.2021.120287 PMID: 33589845

[174] Rangsinth, P.; Sillapachaiyaporn, C.; Nilkhet, S.; Tencomnao, T.; Ung, A.T.; Chuchawankul, S. Mushroom-derived bioactive compounds potentially serve as the inhibitors of SARS-CoV-2 main protease: an *in silico* approach. *J. Tradit. Complement. Med.,* **2021**, *11*(2), 158-172.
http://dx.doi.org/10.1016/j.jtcme.2020.12.002 PMID: 33520685

[175] Sen, D.; Debnath, P.; Debnath, B.; Bhaumik, S.; Debnath, S. Identification of potential inhibitors of SARS-CoV-2 main protease and spike receptor from 10 important spices through structure-based virtual screening and molecular dynamic study. *J. Biomol. Struct. Dyn.,* **2020**, 1-22. Epub Ahead of Print
http://dx.doi.org/10.1080/07391102.2020.1819883 PMID: 32948116

[176] Siddiqui, S.; Upadhyay, S.; Ahmad, R.; Gupta, A.; Srivastava, A.; Trivedi, A.; Husain, I.; Ahmad, B.; Ahamed, M.; Khan, M.A. Virtual screening of phytoconstituents from miracle herb *Nigella sativa* targeting nucleocapsid protein and papain-like protease of SARS-CoV-2 for COVID-19 treatment. *J. Biomol. Struct. Dyn.,* **2020**, 1-21. Epub Ahead of Print
http://dx.doi.org/10.1080/07391102.2020.1852117 PMID: 33289456